CONFIDENTIAL

CaMK1D kinase: a potential target for breast cancer therapy

by Jasmeen Kaur Sethi

UNIVERSITY OF BIRMINGHAM

A thesis submitted to the University of Birmingham for the degree of MRes in Cancer Sciences.

School of Cancer Research
College of Medical and Dental Sciences
University of Birmingham
August 2014

Abstract

Basal like breast cancer (BLBC) is a highly aggressive and invasive subtype of triple negative breast cancer. BLBC patients are offered empirical treatments, which is associated with poor patient prognosis. The recent study of the genomic and transcriptomic background of 2000 breast cancers together with the discovery of a 10p13 chromosomal gain in BLBC suggest that a kinase known as CaMK1D serves as a driver for disease progression. In-house testing of small molecule compounds using structure-based techniques have already exhibited selective inhibition of the CaMK1D oncogenic state locking it in an autoinhibitory state. Here, we developed a cell-based model system for assays required to evaluate these inhibitors *in vitro*. BLBC cell lines, HCC70 and MDA-MB-231, were stably transformed using lentiviral transfections to express varying CaMK1D protein levels; knockdown, basal and overexpression. Western blot analysis of the MDA-MB-231 model system identified potential biomarkers that could serve as a molecular readout of the inhibitor potency. Cytotoxicity and migration assays using the MDA-MB-231 model system proposed that primary inhibitor of interest, GSK-3 XIII, is a not a CaMK1D-specific inhibitor *in vitro*. Thus, the model system generated is appropriate for studying the preliminary *in vitro* effects of CaMK1D inhibition in cell-based assays.

Acknowledgements

I would like to express my sincere appreciation to Professor Michael Overduin for giving me the opportunity to work on this project, his guidance and support throughout my project and for his valuable and speedy feedback with my thesis. My sincere gratitude goes to my mentor Dr Rajesh Sundaresan for his guidance, support, patience and encouragement throughout the research work, and for always having the time to teach me the skills needed to undertake this project. I would like to thank Dr Fedor Berditchevski for patiently taking the time to guide me with the planning and analysis of the experiments and for the constructive feedback.

My deepest gratitude are extended to Dr Elena Odintsova, Vera Novitskaia, Dr Rana Roy and Izabela Bombik for their guidance with experimental techniques and for their help in all the small but incredibly important tasks of my labwork. My heartfelt thanks to Sandya Rajesh for caring for my well-being. I would like to thank Dr Timothy Knowles, Dr Claudia Fogl, Pooja Sridhar, Jaswant Kaur, Lee Quill, Dr Marc Lenoir, Dr Xiaohong Lu and Dawar Pasha for making labwork enjoyable. Above all, for their friendship, which has made this an experience I will cherish forever.

I would like to thank my family and friends for their love, words of encouragement and constant support throughout my undergraduate and graduate degree, and for their faith and support to pursue my academic goals.

Table of contents

Abbreviations

Abl	Abelson
AID	Autoinhibitory domain
Akt	Retovirus strain Ak thymoma
ATP	Adenosine triphosphate
BRAF	b-rapidly accelerated fibrosarcoma
BSA	Bovine serum albumin
Ca^{2+}	Calcium
CaM	Calmodulin
CaMK	Calcium/Calmodulin Kinase
CaMK1D	Calcium/Calmodulin-dependent protein kinase 1D
CaMKK	Calcium/Calmodulin Kinase Kinase
CBD	Calcium/Calmodulin binding domain
CDK9	Cyclin dependent kinase 9
CDKN2A	Cyclin-dependent kinase inhibitor 2A
CKLiK	Calcium/Calmodulin-dependent protein kinase 1-like kinase
CML	Chronic myeloid leukemia
c-Raf	c-rapidly accelerated fibrosarcoma
CREB	cAMP-responsive element binding protein
DMEM	Dulbecco's modified Eagle's medium
DMSO	Dimethyl sulfoxide
EGFR	Epidermal growth factor receptor
EMT	Epithelial-mesenchymal transition
ER	Oestrogen receptor

ER	Endoplasmic reticulum
ERK	Extracellular signal-regulated kinase
GSK-3 XIII	Glycogen synthase kinase-3 XIII
HER2	Human epidermal growth factor receptor 2
HGF	Hepatocyte growth factor
HI-FBS	Heat-inactivated fetal bovine serum
IC_{50}	Half maximal inhibitory concentration
KRAS	k-Rat sarcoma
MAPK	Mitogen-activated protein kinase
MEK	Mitogen/extracellular signal-regulated kinase
NF2	Neurofibromatosis type II
P/S	Penicillin/Streptomycin
p38 MAPK	p38 mitogen-activated protein kinase
PBS	Phosphate buffered saline
PFA	Paraformaldehyde
PKB	Protein kinase B
PKC	Protein kinase C
PR	Progesterone receptor
PTEN	Phosphatase and tensin homolog
RPMI	Roswell Park Memorial Institute
s.e.m	Standard error of the mean
Ser	Serine
SF	Scatter factor
SR	Sarcoplasmic reticulum

Src	Sarcoma
TBST	Tris-buffered saline with Tween 20
Thr	Threonine
TNBC	Triple negative breast cancer
Tyr	Tyrosine

1. Introduction

Cancer (used interchangeably with 'tumour' in this thesis) refers to the development of a mass of cells due to generally uncontrolled division and growth of cells (Hanahan and Weinberg, 2011). These malignant tumour cells can then invade nearby tissues causing damage in that cellular niche. One of the most common and heterogeneous type of cancer is breast cancer; it accounts for about 30% of new cancers in females in the U.K. (Cancer Research UK, 2014). Regardless of similar alterations at the genomic, transcriptomic and proteomic levels, these breast cancer entities display radical variations morphologically and histologically. Subsequently, they respond differently to treatments resulting in varying patient outcomes (Perou et al., 2000). This underpins the need for personalised therapy, which utilises such information to determine appropriate treatment.

1.1 Molecular subtypes of Breast Cancer

Depending on the gene expression pattern, breast cancer can be sub-divided into five molecular types; normal-like, human epidermal growth factor receptor 2 (HER2)-associated, luminal-like Type A, luminal-like Type B and basal-like (Perou et al., 2000) (Figure 1). Of these, it has been particularly hard to target basal-like breast cancer (BLBC) because it is often a triple negative breast cancer (TNBC), i.e. the tumour cells do not express oestrogen receptor (ER), progesterone receptor (PR) or HER2. Consequently, while tamoxifen and Herceptin (a humanised anti-HER2 monoclonal antibody) can be used as a targeted therapy for ER+ and HER2+ cancers, respectively, conventional anticancer agents are not effective against BLBC (Rakha et al., 2008). BLBC are resistant to these drugs and treatments for BLBC rely on a combination of general cell

toxicity drugs, for example, doxorubicin and cisplatin. Thus, the current method of management includes palliative care and treatments that are available to other stage- and grade- matched breast cancers (Rakha et al., 2008).

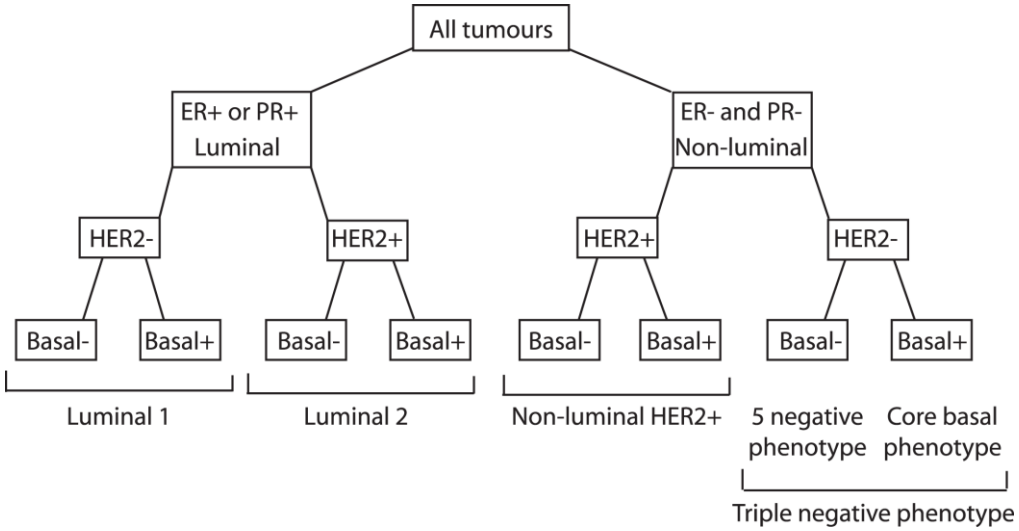

Figure 1. A schematic of molecular subtypes of breast cancer. There are 5 subtypes of breast cancer – basal-like, luminal-like Type A, luminal-like Type B, HER2-associated and normal-like - based on the resemblance of cell type, expression of receptors and other genetic variants (Blows et al., 2010).

BLBC accounts for 12-37% of breast cancers incidences in the U.K. (Toft and Cryns, 2011). Several studies have shown that BLBC is associated with poor patient outcome (Fan et al., 2006). Frequently diagnosed as an interval cancer and as an invasive ductal carcinoma of no special type, BLBC particularly affects the younger, Hispanic or African-American premenopausal females (Majorano et al., 2010). BLBC is so-called because it displays molecular features similar to those of basal or myoepithelial features, including high-molecular-weight cytokeratins - CK5/6, CK14, CK17 - and proteins like P-cadherin (Badve et al., 2011). Additionally, this form

of cancer is also associated with a high mitotic count. Histologically, BLBC is a pushing border tumour and contains necrotic or fibrotic tissues (Majorano et al., 2010). The tumour is proposed to be highly infiltrated with lymphocytes and presents with both typical and atypical medullary features (Badve et al., 2011). Not only does it have high DNA copy number variations, it has been demonstrated that BLBC are often characterised by mutations in BRCA1 mutants (Wang et al., 2010). Hence, this tumorigenic phenotype could be the result of one or more prevalent genetic mutation.

1.2 Genetic causes of BLBC

One of the enabling characteristics of cancer is genomic instability and mutation (Hanahan and Weinberg, 2011). Mutations at the chromosomal level can act as drivers for cancer. Oncogenic genes and loss of tumour suppressor genes can alter the function of proteins, resulting in aberrant signalling. A common copy number variation observed in BLBC is a chromosomal gain at the 10p region (Bergamaschi et al., 2008). Amongst the genes within the smallest chromosomal gain detected in the 10p13 region, the only protein kinase, and therefore potential druggable target, is calcium/calmodulin-dependent protein kinase 1D (CaMK1D) (Figure 2). Although it is proposed to mediate glucose metabolism in hepatocytes (Haney et al., 2013) and is associated with Type II diabetes (Gamboa-Meléndez et al., 2012), CaMK1D is generally an understudied protein and its specific biological role is currently an enigma. CaMK1D is often referred to as CaMK1 like kinase (CKLiK) because CKLiK is considered to be a splice variant of CaMK1D. The expression of CKLiK is well characterised in polymorphonuclear leukocytes, whereas CaMK1D is expressed in a variety of tissues such as the ovaries, liver and brain (Verploegen et al., 2000; Verploegen et al., 2005).

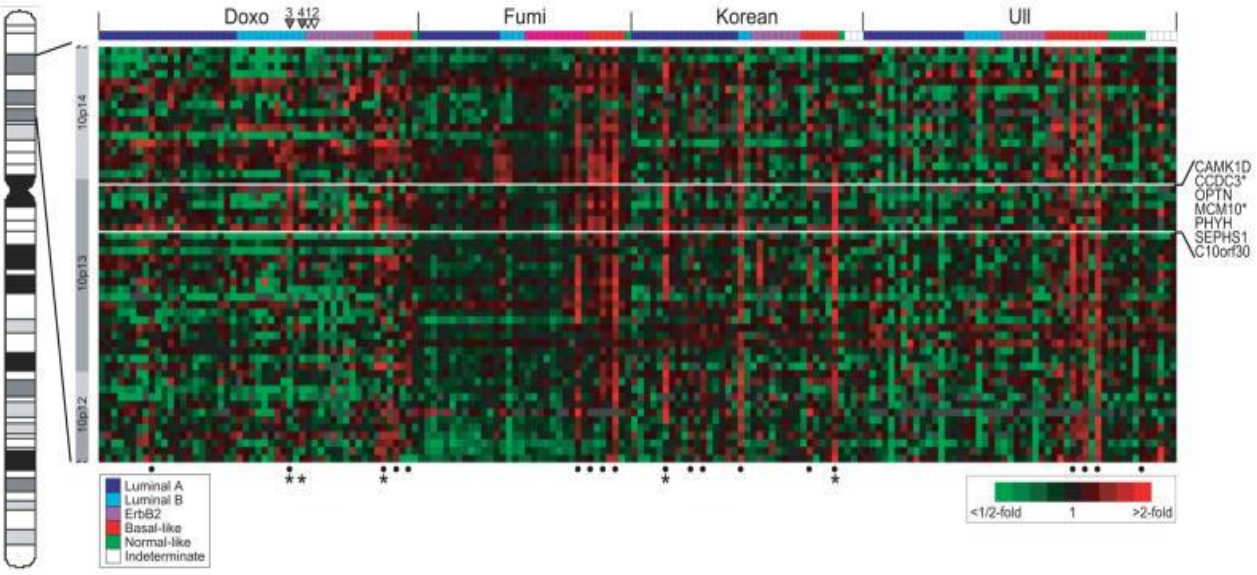

Figure 2. The genomic profile of the 10p13 cytoband of primary breast cancers based on comparative genomic hybridization. A total of 172 breast tumours were obtained from four different cohorts, a Korean cohort and three Norwegian cohorts known as Doxo, Fumi and Ull, and their chromosomal levels studied. The columns of the profile correspond to a distinct tumour, and are organised according to their molecular subtype and cohort. The rows correspond to a distinct gene. Red corresponds to a gain in the tumour sample at the genomic position whereas green represents a loss. The smallest genomic region in BLBCs that demonstrated an overall gain contained 7 genes, one of which is CaMK1D (Bergamaschi et al, 2008).

Interestingly, CaMK1D has been proposed to be a driver for disease progression by a large scale genomic and transcriptomic analysis of 2000 breast cancers (Curtis et al., 2012). A study was conducted in which some of the effects of CaMK1D in BLBC had been characterised. MCF-10A mammary epithelial cells with CaMK1D overexpression have demonstrated to enhance cell proliferation and cell cycle progression (Bergamaschi et al., 2008). CaMK1D overexpression

correlated with decreased E-cadherin expression, reflecting a loss in cell-cell contact. Furthermore, increased expression of vimentin and scratch wound assays demonstrated that CaMK1D overexpression promotes cell migration (Bergamaschi et al., 2008). Altogether, the data proposed that CaMK1D overexpression or hyperactivity promotes an epithelial-mesenchymal transition (EMT), a feature which is characteristic of BLBC progression.

1.3 CaMK1D is a member of the Ca2+-/Calmodulin-dependent kinase signalling pathway

The human CaMK1D protein is comprised of 385 residues with a known molecular weight of 42.9 kDa (Tong, 2011). It functions as a protein kinase, which refers to an enzyme that covalently adds the gamma phosphate group(s) from adenosine triphosphate (ATP) molecules to other proteins in a process known as phosphorylation. This alters the function or location of this phosphorylated target. In response to extracellular physiological or internal stimuli, intracellular signalling events often rely on phosphorylation to convey the signals. Such signalling events are vital for various cellular processes including cell proliferation, cellular metabolism, apoptosis, and gene expression (Dancey and Sausville, 2003). The human genome contains 518 known kinases that are divided into 10 groups; of which one is known as the Calcium/Calmodulin (Ca^{2+}/CaM) Kinase (CaMK) family (Manning and Whyte, 2002). Of the 80 members in this family, each subfamily of these Serine/Threonine (Ser/Thr) kinases contain a N-terminal kinase catalytic domain followed by an autoinhibitory domain (AID) in the C-terminal region that is contiguous to and overlap part of a Ca^{2+}/CaM binding domain (CBD) (Swulius and Waxham, 2008). Thus, the activation of these kinases intrinsically depends on Ca^{2+} signalling.

Ca^{2+} interactions are vital for countless signalling pathways in all cell types. The concentration of cytosolic Ca^{2+} generally increases due to the increase of transport of extracellular Ca^{2+} *via* Ca^{2+} transporters or Ca^{2+}- channels or due to the release of Ca^{2+} from intracellular stores, for example, the sarcoplasmic and endoplasmic reticulum (SR & ER) (Berridge et al., 1998). Calcium can act as a secondary messenger and can interact with downstream Ca^{2+} binding proteins to facilitate events including cell proliferation and apoptosis. CaM is known as a Ca^{2+} sensor and is one of such binding proteins that is highly conserved in all eukaryotic cells and contains four Ca^{2+}-binding sites. To activate this Ca^{2+} sensor, the binding of at least two Ca^{2+} ions to CaM is required to induce a conformational change associated with ligand binding (Berridge et al., 1998).

Some of the more indirect effects of Ca^{2+} are facilitated by the CaM kinase family of proteins. Ca^{2+}/CaM is an allosteric activator of CaMK proteins. In the absence of Ca^{2+}/CaM, these Ser/Thr kinases adopt a relatively inactive state in which the AID folds over and conceals the catalytic cleft. The binding of Ca^{2+}/CaM to the CBD relieves the kinase of its autoinhibitory state. This exposes the catalytic cleft and the kinase adopts an active state allowing it to phosphorylate the Ser/Thr residues on CaMK substrate proteins (Hook and Means, 2001). Full activation of these CaMK proteins involves not only Ca^{2+}/CaM binding but also a CaMK protein- mediated phosphorylation of the activation loop. The basal level of CaMK1D activity is stimulated by Ca^{2+}/CaM binding, however, a 30-fold increase in activity has been reported upon the addition of an upstream kinase, CaMKK (Ishikawa et al., 2003). In the presence of Ca^{2+}, CaM binds to and aids the activation of CaMKK (Figure 3). This activated kinase can then phosphorylate the activation loop of CaMK1D at Thr180 (Ishikawa et al., 2003). Enhanced activation of CaMK1D

is proposed to lead to phosphorylation of downstream targets, for example, cyclin dependent kinase 9 (CDK9), which can modulate RNA Polymerase-II mediated transcription (Ramakrishnan and Rice, 2012).

Most of the members of the CaMK family of kinases are localised to the cytoplasm, however it has been reported that CaMK1D translocates to the nucleus upon a stimulus, for example, Ca^{2+} influx (Sakagami et al., 2005). There, it may phosphorylate the cAMP-responsive element binding protein (CREB) (Kimura et al., 2002), a ubiquitous transcription factor that regulates transcription of genes involved in cell growth and differentiation (Shaywitz and Greenberg, 1999). Subsequently, this decreases E-cadherin expression and increases vimentin expression, which can decrease cell adhesion and increase cell migration, respectively (Bergamaschi et al., 2008). The members of the CaMK family can remain in constitutively active state even following decay in the Ca^{2+} signals due to their ability to autophosphorylate. To return these kinases to their basal activity, Ser/Thr phosphatases are required to remove the activating phosphates from the phosphorylation sites (Soderling and Stull, 2001).

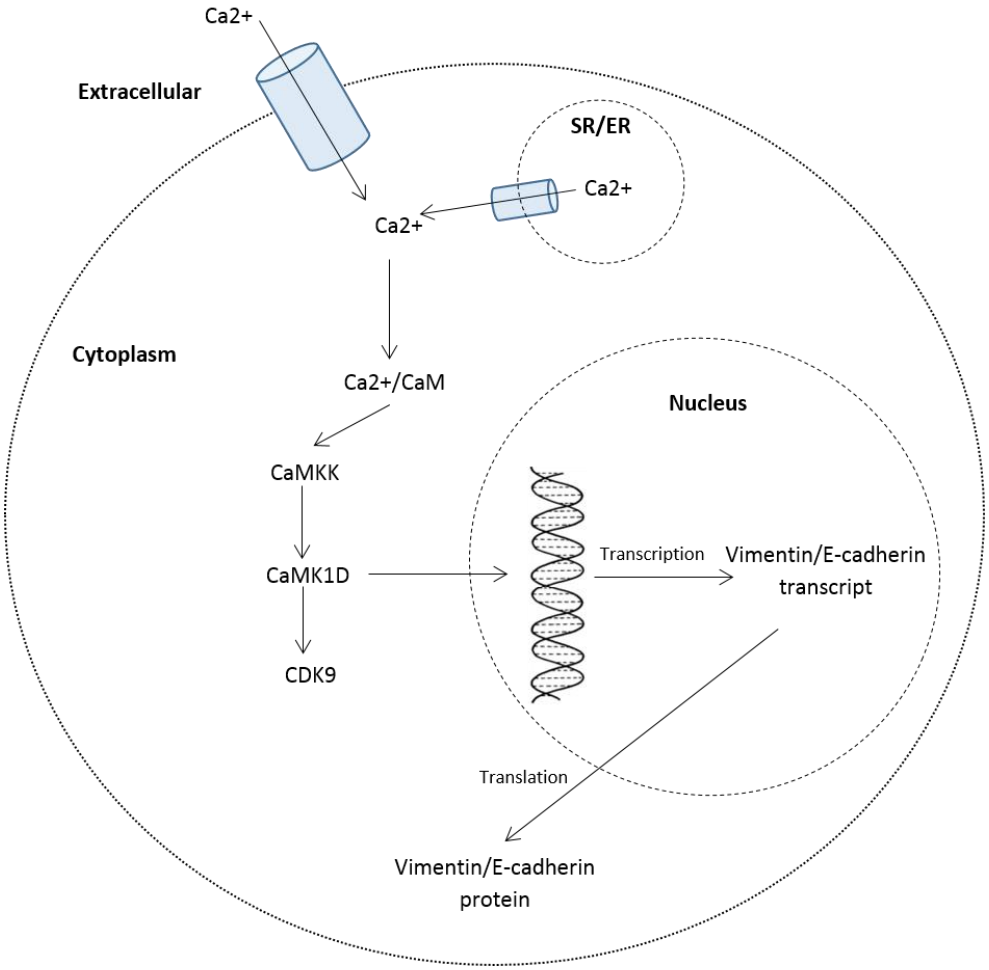

Figure 3. A schematic of the proposed Ca^{2+} signalling pathway involving CaMK1D. Extracellular Ca^{2+} and/or Ca^{2+} from the SR/ER stores bind to CaM in the cytoplasm. Together they bind to activate CaMKK. Ca^{2+}/CaM binding and CaMKK-dependent phosphorylation activates CaMK1D, which can phosphorylate CDK9 and translocate to the nucleus. In an unknown mechanism, CaMK1D is proposed to bind to CREB and mediate the transcription of genes such as vimentin and E-cadherin.

1.4 CaMK1D as a druggable target

'The druggable genome' refers to the human genes coding for proteins that can be targeted by drug-like compounds, of which 22% are Ser/Thr and Tyr protein kinases (Hopkins and Groom, 2002). Although a protein target is considered potentially druggable if it exhibits a reasonable binding affinity with a small molecule compound, it is only considered as a drug target if it is associated with a disease and the efficacy of lead molecules have been demonstrated. One of the most successful mechanism-based drug molecules is Imatinib or Glivec, an inhibitor developed to target an oncogenic tyrosine kinase overexpressed in chronic myeloid leukemia (CML) (Capdeville et al., 2002). It attained acceptable drug specificity because only the oncogenic, constitutively active form of the kinase is expressed during disease progression and is distinguishable from the tightly regulated activity of the normal form of the enzyme found in non-transformed cells. Successful drug discovery relies on the iterative modification and testing of a series of lead compounds that exhibit an acceptable balance of cellular activity and minimal off-target toxicity. This is achieved through medicinal chemistry optimization to engineer in specificity, affinity and drug-like properties. A protein kinase C inhibitor was the lead compound for Glivec, which was processed further using medical chemistry by the addition of certain derivatives (Capdeville et al., 2002). These modification fulfilled the requirements for an effective small molecule therapeutic agent with minimal drug-drug-interactions that expresses the appropriate absorption, distribution, metabolism and excretion features. Thus, in the end Glivec was successfully developed for cancer treatment as a water soluble compound with good oral bioavailability (Capdeville et al., 2002), and demonstrated a way forward for the development of additional kinase inhibitors as selective anti-cancer agents.

Bergamaschi and colleagues proposed that the Ser/Thr kinase hyperactivity of CaMK1D acts as a breast cancer driver (Bergamaschi et al., 2008), suggesting that its enzymatic activity is an appealing drug target. Similarly to Glivec, a screen relevant to the cancer must be conducted to identify and progress the CaMK1D inhibitors as potential lead compounds for this novel target. Substrate- or ATP- binding sites within a protein are generally functionally relevant, thus small molecule inhibitors competing for such binding sites ($K_D \leq 10\mu M$) to induce a toxic effect are deemed to be effective. Previous research carried out by the groups of Stefan Knapp (University of Oxford) and Michael Overduin (University of Birmingham) showed the interaction between kinase inhibitors and CaMK1D using X-ray crystallography and NMR techniques. Since most kinase inhibitors are ATP analogues (Rinnab et al., 2008), the inhibitors were generally expected to occupy the ATP-binding site of CaMK1D. The inhibitor of initial interest, which is commercially available, was glycogen synthase kinase (GSK)-3 XIII. It was originally developed as an inhibitor of the GSK3 kinase (Rinnab et al., 2008), which is implicated in several physiological functions that involve cell proliferation and cell death (Takahashi-Yanaga, 2013). This inhibitor can also bind to CaMK1D to cause an autoinhibitory effect on the kinase by locking it in an autoinhibitory state, as viewed in the 2.3Å inhibitor complex crystal structure (Figure 4). Thus, by designing effective and specific inhibitors of CaMK1D one can lay the basis for developing targeted systemic treatment for BLBC patients.

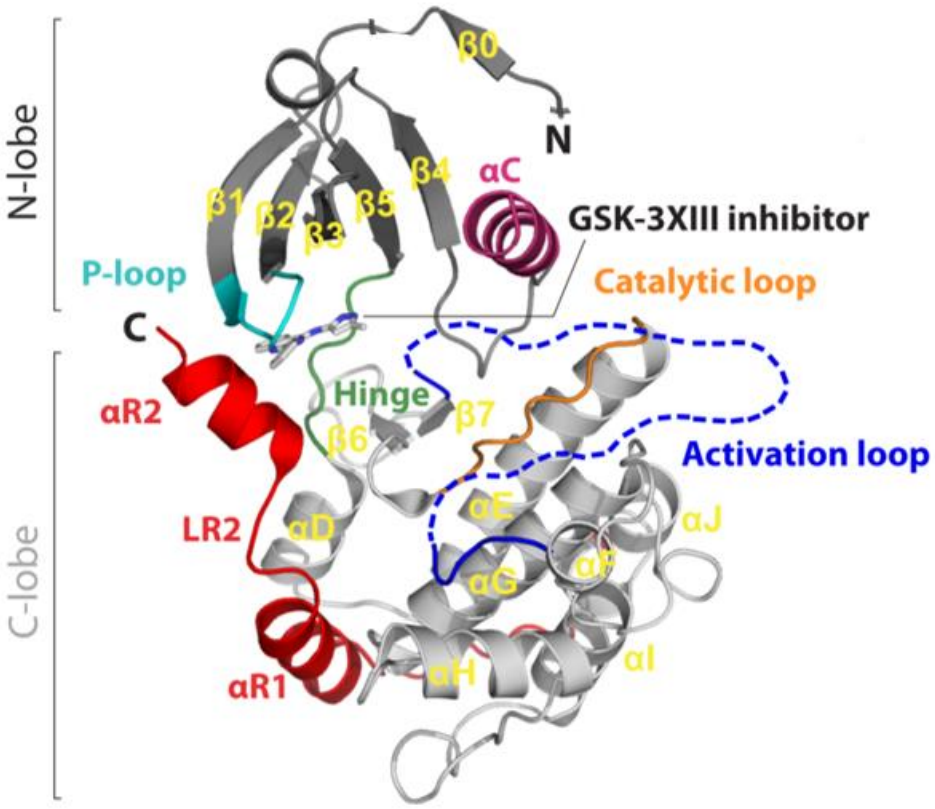

Figure 4. Crystal structure of CaMK1D with GSK-3 XIII inhibitor. (PDB:2JC6) The GSK-3 XIII inhibitor is bound to the ATP binding site within the N-lobe of this monomeric CaMK1D, thereby locking the AID (denoted as αR1 and αR2) within the C-lobe (Figure provided by Stefan Knapp, University of Oxford).

One of the unusual attributes which accounts for the success of Glivec is that CML disease progression results from only one aberrant signalling pathway event. In contrast, the majority of tumours are the result of several deregulated proteins involved in multiple signalling pathways. Although, the exact biological pathway involving CaMK1D in cancer cells is poorly understood, CaMKK and CaMK1V have been reported to indirectly activate Protein Kinase B (PKB) and members of the MAPK/ERK pathway, respectively (Soderling, 1999; Means, 2000). However,

other components of diverse pathways may also be affected. Furthermore, the generally high sequence homology within members of the CaMKK family suggests that their binding sites and specificities could be conserved, allowing a single compound to bind several related members. Previously, it has been demonstrated that a CaMKII inhibitor- KN93- and siRNA can inhibit CaMKI by triggering cell cycle arrest and reducing cell proliferation in adenocarcinomic MCF-7 cells (Rodriguez-Mora, 2005). This suggests that members of the same family can be targeted by the same inhibitor. There are 4 known isoforms of kinases in the CaMK1 subfamily – CaMK1A, CaMK1B, CaMK1D and CaMK1G. The sequences of these isoforms are highly conserved throughout the kinase except at the C-terminus region following the AID (Ishikawa et al., 2003). The inhibitors that target the catalytic or AID or such domains could be translated to other kinases due to limited sequence diversity. On the other hand, off targets should be avoided to achieve tumour selectivity. This highlights the requirement of generating a model system to study the drug's specificity for the target, i.e. CaMK1D, as well as a series of off-targets such as related CaMKK family members.

1.5 Targeting CaMK1D as a form of targeted therapy for BLBC

The method of screening a series of compounds for modulation of an established disease target is known as a targeted drug discovery. To conduct this process under *in vitro* conditions, it is essential to develop a cell-based model system designed to test the effects of the compounds on cells expressing various CaMK1D levels in different tumorigenic backgrounds corresponding to different states of the disease progression. Upon the generation of this model system, several cell-based assays should be conducted as readouts of an inhibitor's specificity and potency in the cancer cell model as well as other tissues where toxic side-effects could be anticipated.

2. Aims of the Project

- **To establish a cell-based model system to test for specific inhibitors against CaMK1D.**

  This will be achieved by generating a panel of stably transformed cell lines (referred to as 'model system') with three different CaMK1D expression levels - knockdown, basal and overexpression- to test for the inhibitors' specificity. We predicted that inhibitors targeting CaMK1D under basal and overexpression conditions would recapitulate the phenotype observed under the CaMK1D knockdown condition. Comparison of effects at basal and overexpression conditions also allows us to determine if the inhibitor is CaMK1D-specific or exhibits off-target effects.

- **To determine the relevant downstream targets of CaMK1D that can serve as biomarkers for CaMK1D-specific inhibitors.**

  This will be achieved by western blot analysis of predicted CaMK1D substrates and associated signalling pathways, based on the literature available.

- **To perform cell-based assays for the evaluation of the *in vitro* effects by the inhibitors and the identification of potential CaMK1D-specific lead compounds.**

  This will be achieved by performing cytotoxicity and wound-healing assays, which will determine the binding affinity of the compound, and inhibitory effects on cell migration and invasion respectively. This would reflect the specificity and potency of the inhibitor under these varying CaMK1D expression levels.

3. Material & Methods

3.1 Plasmid DNA isolation

In order to generate cell lines with varying CaMK1D expression levels, the following ampicillin–resistant plasmids were amplified and purified: pLVX, HA-tagged CaMK1D, sh1753, sh1754, sh95712, sh97125, pSPAX and pMD2.G (Sigma-Aldrich). Bacterial transformation was carried out by thawing 40µl of competent *E.coli* DH5α cells (Life Technologies) on ice prior to the incubation with 2µl of the 1µg/µl plasmid for 5 minutes on ice. The DH5α cells underwent a 30-second heat shock at 42˚C, followed by a 2-minute incubation on ice. The cells were then incubated at 37˚C for an hour with 250µl of SOC (Novagen) pre-warmed to room temperature on a shaker at 220rpm. 80µl of this mixture was plated onto an LB agar plate containing ampicillin pre-warmed to room temperature. The plate was inverted and cells were incubated overnight at 37˚C. Pre-autoclaved LB media (1ml) was added to the agar plate and mixed with a spreader. This step was performed twice before the media containing cells from the colonies was used to inoculate a 500ml LB medium with ampicillin at 37˚C and 60rpm overnight. The culture was harvested once it appeared to be turbid with an OD reading of 600nm. DNA was isolated using the Plasmid Maxi Kit (QIAGEN) according to the manufacturer's instructions. The purified plasmids were then used to transfect human cell lines.

3.2 Cell culture

Human cell lines were tested for effects of CaMK1D expression and inhibition. These included HEK 293T (ATCC:-LGC) and MDA-MB-231 (ATCC:-LGC) cells, which were cultured in Dulbecco's modified Eagle's medium (DMEM) (Gibco) containing 1% Penicillin/Streptomycin

(P/S) (Gibco) and 10% heat-inactivated Fetal Bovine Serum (HI-FBS) (Gibco). HCC70 (ATCC:-LGC) cells were cultured in Roswell Park Memorial Institute (RPMI) 1640 medium (Gibco) containing 1% P/S (Gibco) and 10% HI-FBS (Gibco). All these cell lines were grown and maintained at 37˚C and 5% CO_2 in an incubator with 95% humidity.

3.3 Cell transfections

3.3.1 Transient transfections

The HEK 293T cells were grown to 80-90% confluency for plasmid transfections. A transfection volume of 8µl of plasmid and 12µl of polyethylenimine (Sigma-Aldrich) was vortexed and incubated in 1ml of serum-free media for 15 minutes at room temperature prior to their addition to HEK 293T cells. This was performed with each of the following plasmids: pLVX, HA-tagged CaMK1D, sh1753, sh1754, sh95712, sh97125. These cells were then grown in DMEM containing 2% FBS with the transfected solution for 8 hours before the media was replaced with 10% serum-containing media. These cells were cultured for 40 hours prior to lysis.

3.3.2 Lentiviral transfection

Lentiviral transductions were performed on two cell lines of interest, HCC70 and MDA-MB-231. Thus, the following procedure was performed three times. Packaging cells, i.e. HEK 293T, were grown to 80-90% confluency preceding plasmid transfections. A transfection volume of 8µl of plasmid, 12µl of pSPAX and 12µl of pMD2.G was vortexed and incubated in 1ml of serum-free media for 15 minutes at room temperature prior to their addition to the packaging cells. This was performed with each of the following plasmids; pLVX, HA-tagged CaMK1D, sh1753, sh1754, sh95712 and sh97125. The cell lines to be transfected with the infective virus were also grown to

80-90% confluency preceding viral transfections. At 24 hours and 48 hours post-transduction, the viral particles suspended in the media of these packaging cells were filtered. Infective virus containing pLVX and HA-tagged CaMK1D were directly added to the cell line of interest whereas infective virus containing sh1753, sh1754, sh95712 and sh97125 were pooled and collectively added to the cell line of interest. At 48 hours post this viral transfection, the media was replaced with media containing 2mg/ml puromycin (Fisher Scientific) to select for stable transfectants.

3.4 Cell morphology imaging

3.4.1 Morphology of the 2D culture

Cells were plated at a density of $8.0x10^5$ onto 60mm dishes and incubated for 48 hours. Upon attaining 80-90% confluency, cells were imaged using Axiovert S 100 microscope (Zeiss) at 10X magnification with the Scion Image software (Scion Corporation).

3.4.2 Morphology of the 3D culture

Thaw matrigel (BD Biosciences) on ice. 50µl of 100% matrigel was spread onto each well of an 8-well glass Nunc Lab-Tek Chamber Slide (Thermo Scientific), placed on ice. This Chamber Slide was placed on a rocker for 5 minutes prior to placing it in an incubator. $1x10^4$ cells in 200µl were mixed in a 1:1 ratio of cells to 8% matrigel in media. This mixture was plated into each chamber of the Chamber Slide and incubated for 5 days. Upon attaining sufficient colonies, 400µl of 4% paraformaldehyde (PFA) was added to each well and incubated for 15 minutes at room temperature. Then the PFA was removed and replaced with fresh PFA. This was left to incubate overnight at 4˚C. The PFA was removed and 400µl of phosphate buffered saline (PBS)

containing 10% azide was added to every chamber. The Chamber Slide was sealed with parafilm until imaging. Images were taken on Axiovert S 100Z microscope with the Scion Image software at 10X magnification.

3.5 Cell lysis

Cultured cells from the transient and lentiviral transfections were incubated on ice for 5 minutes before washed trice with cold PBS. Subsequently, they were lysed with 1x Laemmli buffer containing 1x PhosSTOP (Roche EASYpack) and 2x Protease inhibitor (Roche EASYpack) for 5 minutes on ice. Cells were then scraped into an eppendorf and sonicated at 10 microns (Soniprep 150). These lysates were centrifuged for 7 minutes at 14000rpm and at 4˚C. The supernatant was removed and boiled at 95˚C for 5 minutes.

3.6 Western Blot

The protein levels in the lysates prepared from the cell transfections and lysates of other cell lines previously prepared were quantified using DC Protein Assay (BioRad) on a 96-well plate (BD Falcon) according to the manufacturer's instructions. A DC iMark microplate reader (BioRad) was used to measure the absorbance of the assay at 750nm. For identification by gel electrophoresis, 15-20µg of proteins with 5x reducing Laemmli buffer were loaded onto 4-12% TGX precast gels (BioRad). Gels were transferred onto PVDF membranes (BioRad) within 7 minutes using the TransBlot Turbo Transfer System (BioRad). Membranes to be tested with antibodies targeting the phosphorylated forms of proteins were blocked in 3% bovine serum albumin (BSA) in 1x Tris-Buffered Saline with Tween 20 (TBST) whereas those targeting the non-phosphorylated forms of proteins were blocked using 5% milk 1xTBST for 1 hour. This was

followed by an overnight incubation at 4˚C with primary antibodies (Table 1). Primary antibodies were removed and membranes subjected to three 10-minute washes with 1xTBST. They were then incubated with secondary antibodies (LiCor Odyssey) diluted 1:20 000 in appropriate blocking solution, which included fluorophore-attached Goat anti-Rabbit and anti-Mouse, for 1 hour at room temperature. Secondary antibodies were removed and membranes were subjected to three 10-minute washes with 1xTBST. Blots were processed using Gel Imaging Scanner (LiCor Odyssey).

Antibody	Dilution	Clonality	Source	Manufacturer
CaMK1D	1:10 000	monoclonal	rabbit	Abcam
Syntenin-1	1:1000	monoclonal	rabbit	Abcam
Phospho- syntenin-1 Ser6	1:1000	polyclonal	rabbit	Generated "in-house"
Phospho-syntenin-1 Tyr4	1:1000	polyclonal	rabbit	Generated "in-house"
Phospho-syntenin-1 Tyr47	1:1000	polyclonal	mouse	Generated "in-house"
E-Cadherin	1:100	monoclonal	mouse	Abcam
Vimentin	1:1000	polyclonal	rabbit	Abcam
Phospho-CREB Ser133	1:1000	monoclonal	rabbit	Cell Signaling
Phospho-Ser	1:1000	polyclonal	rabbit	Abcam
Phospho-Thr	1:1000	polyclonal	rabbit	Zymed
EGFR	1:1000	monoclonal	mouse	Neomarkers
MEK1/2	1:1000	polyclonal	rabbit	Cell Signaling
ERK1/2	1:1000	polyclonal	rabbit	Cell Signaling
p38 MAPK	1:1000	polyclonal	rabbit	Cell Signaling
β-actin	1:30 000	monoclonal	mouse	Sigma-Aldrich

Table.1. Details of the primary antibodies used for western blot analysis. Listed are the details of primary antibodies used for the characterization of the MDA-MB-231 model system. These antibodies were diluted in 1x TBST containing 3-5% BSA and 0.01% azide

3.7 Proliferation Assay

In order to understand the effect on CaMK1D expression on proliferation, exponentially growing cells were plated onto COSTAR 96-well plates (Corning) with 100µl of the appropriate media. The experimental wells contained cells with media whereas the control wells contained media only. The experimental and control conditions were plated in triplicates. To optimise cell seeding density, the experimental conditions were cells plated at 10 different cell densities, ranging from 7.8x10 to $4.0x10^4$ at a 2-fold difference in media containing 10% FBS, prepared by serial dilution. To optimise serum conditions, cells were plated a $5.0x10^4$ density in serum-free media 24 hours prior to being subjected to the experimental conditions, which were four different serum concentrations; serum-free, 1% FBS, 3% FBS and 10% FBS. Fresh media containing Alamar Blue (Life Technologies) was added in a 10-fold dilution to all wells 4 hours prior to the required time of proliferation reading. Plates were read at 0, 24, 48, 72, and 96 hours, with the 0 hour time-point being 4 hours after the cells were seeded. The fluorescence resulting from the reduction of Alamar Blue was measured using Wallac 1420 VICTOR2 V microplate reader (Perkin Elmer) and Wallac 1420 Manager software (Perkin Elmer) with the excitation and emission wavelength at 560nm and 590nm respectively. The experiment was carried out three times. The mean of the control wells was subtracted from the mean of its respective experimental wells. The adjusted mean values of the three experiments were then calculated and plotted.

3.8 Cytotoxicity Assay

3.8.1 Cytotoxicity Assay performed on HCC70 cells

In order to test the cellular activity of the CaMK1D inhibitor on proliferation, exponentially growing cells were plated at $4x10^3$ cell density onto COSTAR 96-well plates with 100µl RPMI

containing 10% FBS and cultured for 72 hours. The experimental conditions were cells containing different GSK-3 XIII inhibitor (Calbiochem) concentration in 1% dimethyl sulfoxide (DMSO) (Sigma-Aldrich), ranging from 0.001 to 100 µM each with a 10-fold difference. Experimental wells contained cells exposed to the inhibitor whereas controls were exposed to 1% DMSO. The experimental and control conditions were plated in triplicates. Alamar Blue was added in a 1:10 dilution to all wells 4 hours prior to the required time of proliferation reading. Plates were read 48 hours after exposure to the inhibitor using PHERAstar Plus microplate reader (BMG LABTECH) with MARS data analysis software (BMG LABTECH) with the excitation and emission wavelength at 560nm and 590nm respectively. The mean of the control wells was subtracted from the mean of the respective experimental wells and was plotted based on a 4-parameter logistic regression model.

3.8.2 Cytotoxicity Assay performed on MDA-MB-231 cells

Exponentially growing cells at $5x10^3$ density were plated onto COSTAR 96-well plates with 100µl DMEM. Experimental wells contained cells exposed to 10µM of GSK-3 XIII inhibitor in 1% DMSO whereas controls were cells exposed to 1% DMSO. The experimental and control conditions were plated in triplicates. Together with 10µl of Alamar Blue reagent, fresh media containing 10µM of GSK-3 XIII inhibitor and 1% DMSO was replaced in the experimental and control wells, respectively, 4 hours prior to the required time of proliferation reading. Plates were read at 0, 24, 48, 72, 96, 120 and 144 hours, with the 0 hour treatment time-point being 4 hours after the cells were seeded. Plates were read using Wallac 1420 VICTOR2 V microplate reader and Wallac 1420 Manager software with the excitation and emission wavelength at 560nm and 590nm respectively. The experiment was carried out three times. The mean of the control wells

was subtracted from the mean of its respective experimental wells. The adjusted mean values of the three experiments were then calculated and plotted.

3.9 Migration Assay

In order to test the cellular activity of the CaMK1D inhibitor on migration, cells were plated in media containing 10% FBS at a cell density of $2.1x10^4$ cells per chamber of the Culture-Insert migration dish (Ibidi). These were incubated to attach and develop a confluent layer overnight. The media was removed prior to the removal of the Culture-Insert unit. Media containing 10μM GSK-3 XIII and 1% DMSO was added to the experimental and control migration dishes respectively. Images were taken at 10X objective on Eclipse TS100 microscope (Nikon) using QCapture software (QImaging) at 0, 6 and 24 hours.

3.10 Statistical analysis

Standard error of the mean (s.e.m) was provided for experiments performed three times. The P values for data analysis were calculated using Student's *t* test (2-tailed test with 2 sample of equal variance) on Microsoft Excel 2013. Data with P values < 0.05 were considered to be statistically significant and denoted as "*" whereas P values < 0.005 were considered to be statistically very significant and denoted as "**".

4. Results

4.1 Validation of CaMK1D protein expression in human tumour-derived cell lines

Evaluation of CaMK1D expression across a variety of human breast cancer lines only reported the level of CaMK1D transcripts present in the cells. This is insufficient as the microarray data does not reflect the translational efficiency of these transcripts and subsequently the level of CaMK1D protein expression. Hence, a panel of cell lines with varying molecular characteristics (Kao et al., 2009) were selected (Table 2) and analysed for the expression of CaMK1D by western blot (Figure 5). Human kidney epithelial HEK 293T cells transfected with an HA-tagged CaMK1D plasmid was used as a positive control. Not only was CaMK1D expressed in the mammary luminal epithelial HB2 cell line and the lung adenocarcinoma A549 cell line, it was also detectable in the following tumour-derived cell lines; HCC70, ZR75-1, T47D, MD-IBC3, GI 101, CAMA-1, Sum52 and BT474. Thus, any of these tumorigenic human breast cancer cell lines could be used to generate a cell-based assay system.

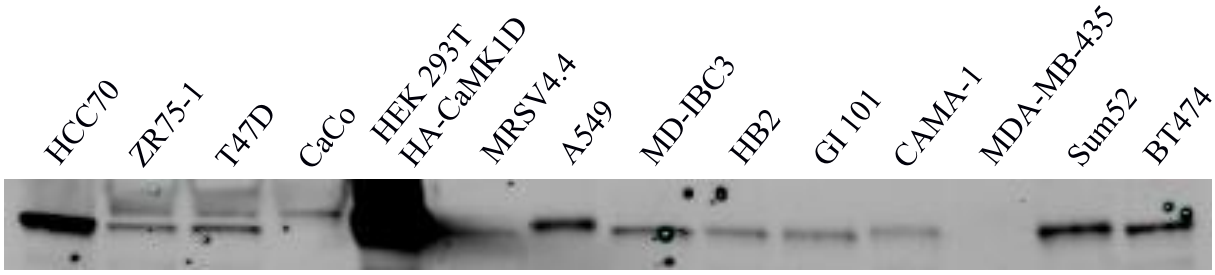

Figure 5. Western blot analysis of CaMK1D expression in a series of cell lines. This blot confirms that the CaMK1D protein is expressed in HCC70, ZR75-1, T47D, A549, MD-IBC3, HB2, GI 101, CAMA-1, Sum52 and BT474 cell lines.

CELL LINE	CELL LINE CHARACTERISTIC
HCC70	Basal-like triple negative breast primary ductal carcinoma cells
ZR75-1	Luminal-type ER+ breast invasive ductal carcinoma cells
T47D	Luminal-type ER+ PR+ invasive breast ductal carcinoma cells
CaCo	Colorectal adenocarcinoma cells
HEK 293T HA-CAMK1D	Kidney epithelial cell transfected with HA-tagged CaMK1D plasmid
MRSV4.4	SV40 immortalization cells acquired from human milk
A549	Adenocarcinomic alveolar basal epithelial cells
MD-IBC3	Inflammatory breast cancer cells
HB2	MTSV1-7 mammary luminal epithelial cells isolated from human milk
GI101	Breast metastatic carcinoma cells
CAMA-1	Luminal-type human breast cancer cells
MDA-MB-435	Breast metastatic carcinoma
SUM52	Luminal-like ER+ & HER2+ breast metastatic carcinoma
BT474	Luminal- like ER+ PR+ HER2+ breast invasive ductal carcinoma

Table 2. A list of cell lines selected for analysis of CaMK1D expression by Western blot. Tumorigenic and non-tumorigenic cell lines of various molecular subtypes and disease stages were tested for the presence for CaMK1D protein. All cell lines were human-derived tumours or originated from human milk.

4.2 Selection of cell lines and evaluation of the constructs used for the generation of the cell-based model system

The above panel of tumorigenic cell lines generally exhibit mutations in several proteins resulting in numerous aberrant signalling pathways. Studying the effects of CaMK1D amidst a single tumorigenic background may not be translatable to other tumorigenic states. To tackle this issue, we aimed to establish model systems from two triple-negative BLBC cell lines that express different basal levels of CaMK1D expression – high and low. The cell line selection was based on the mRNA levels presented by Curtis and colleagues (2012) and on the results of the western blot analysis of CaMK1D protein expression (Figure 5). The first cell line selected was HCC70, which had the highest reported level of CaMK1D mRNA expression (Kao et al., 2009). The cell line selected for its low reported CaMK1D mRNA expression was MDA-MB-231.

The cell-based model system was comprised of a panel of three stably transformed cell lines with varying CaMK1D expression levels; an empty vector control, a CaMK1D overexpressed and a CaMK1D knockdown. This required three different types of DNA constructs that affect CaMK1D protein expression. An empty vector pLVX plasmid was selected to develop the control cell line. An HA-tagged CaMK1D plasmid was selected for the generation of the CaMK1D overexpression line. Combination of four CaMK1D-specific shRNAs- sh1753, sh1754, sh95715 and sh97125- were selected for the generation of the CaMK1D knockdown line. To validate the efficiency of these constructs prior to performing the lentiviral transfection, the plasmids were transiently transfected into HEK 293T cells as they transfect readily (Figure 6). Actin served as loading control. Western blot analysis validated that the HA-tagged CaMK1D plasmid successfully overexpressed CaMK1D. The shRNAs effectively targeted CaMK1D

resulting in a decrease of CaMK1D expression albeit the extent of protein knockdown varied. The sh97125 RNA yielded the highest level of knockdown whereas sh1754 displayed the lowest level of knockdown. Nonetheless, these four shRNAs can be used together to generate the stable CaMK1D knockdown cell line.

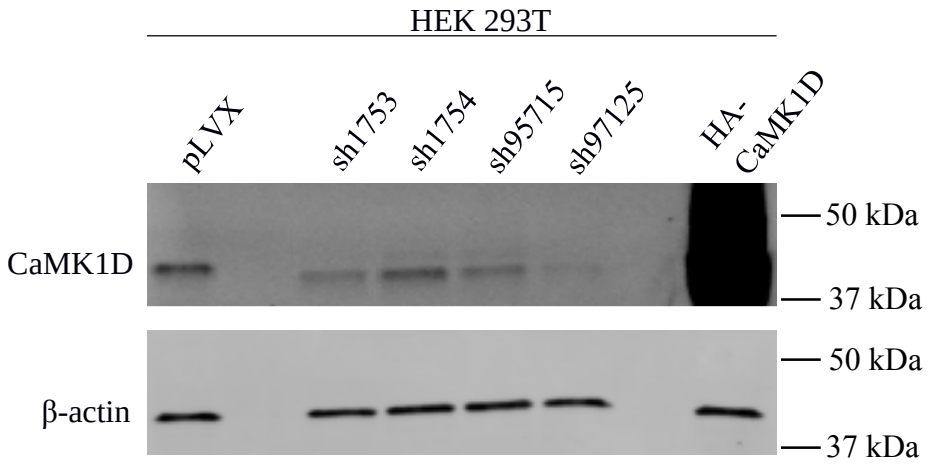

Figure 6. Western blot analysis validating the efficiency of the constructs to be used for the generation of the cell-based assay system. The empty vector pLVX reported the basal level of CaMK1D expression in HEK 293T cells. The four shRNA- sh1753, sh1754, sh95175, sh97125- plasmids downregulated CaMK1D expression when compared to cells expressing pLVX. Transfection of HA-tagged CaMK1D upregulated CaMK1D in HEK 293T cells. Actin served as loading control.

4.3 Establishment of the two cell-based assay systems

Stably transfected lines for the cell-based assay systems were generated to investigate and characterize the effects of CaMK1D at varying expression levels amid different tumorigenic backgrounds. This was achieved with lentiviral transfections of the validated constructs into HCC70 and MDA-MB-231 cell lines as described in the Materials and Methods. Successfully transformed cells were collectively selected with puromycin. After two weeks of puromycin selection, morphological differences were observed in the HA-tagged CaMK1D overexpression line, and the shRNA CaMK1D knockdown line compared to the empty vector control line (Figure 7). Cells were grown on plastic for 48 hours prior to imaging. HCC70 transfected with the empty vector displayed a morphological feature reflective of its epithelial nature. HCC70 shared features of a fibroblast-like appearance that is spindly and multi-polar. Empty vector transfected MDA-MB-231 cells had a fibroblast-like appearance that was generally bipolar. However, in both of the cell-based model systems, cells overexpressing CaMK1D appeared to form colonies in tight cohesive clumps with cells growing in vertical layers. Contrastingly, the CaMK1D knockdown cells appeared to be more elongated and flatter, with colonies growing in loose cohesive monolayers that were spread out. These differences in morphology serve as a primary indicator that these two panels of cell lines were successfully transfected and could be characterised further.

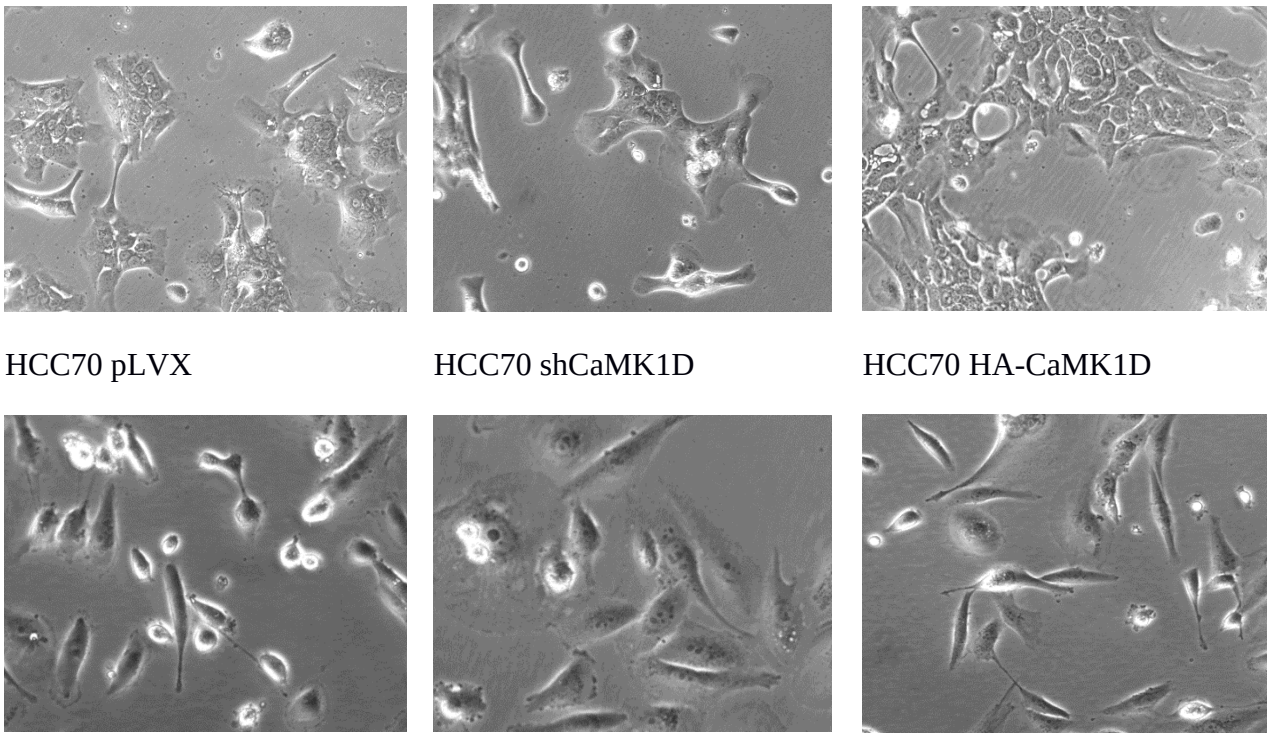

Figure 7. Morphology of the stably transfected lines of the BLBC cell-based model systems in 2D culture at 20X magnification. The HCC70 (top) and MDA-MB-231 (bottom) panel of transformed cell lines with empty vector, CaMK1D knockdown and CaMK1D overexpression. Overall, CaMK1D knockdown resulted in flatter cells that spread out to form a monolayer compared to the morphology observed at basal CaMK1D expression whereas CaMK1D overexpressing cells grew in cohesive clumps.

4.4 Characterisation of the biological pathway involving CaMK1D and identification of potential biomarkers

The generation of a cell-based model system allows for the testing of a library of compounds against CaMK1D, however, validated biomarkers that serve as a readout of the potential inhibitors have not yet been identified. This is largely because the CaMK1D-dependent biological signalling pathway remains understudied. Potential biomarkers could be direct or indirect downstream proteins with expression levels that correlate to the CaMK1D expression levels. To identify such biomarkers, the initial characterisation of these stably transfected cell lines was conducted through western blot analysis. The model system to be cultured and maintained well enough for several cell-based experiments was the MDA-MB-231 panel of transformed cell lines. In these analyses, the pLVX transformed line served as the control, as it reflected the basal levels of proteins in the MDA-MB-231 cell line. Actin served as loading control. Western blot analysis confirmed that CaMK1D was effectively suppressed in the shRNA transfected MDA-MB-231 line (Figure 8). Compared to the basal level expressed by the vector transfected line, the CaMK1D overexpression line displayed approximately a 19-fold increase in CaMK1D expression. Additionally, it is has been proposed that CaMK1D overexpression results in increased vimentin levels and decreased E-cadherin levels (Bergamaschi et al., 2008), which is a characteristic of the EMT phenotype. However, no apparent changes were observed in the expression of vimentin or E-cadherin between the cell lines tested here (Figure 9).

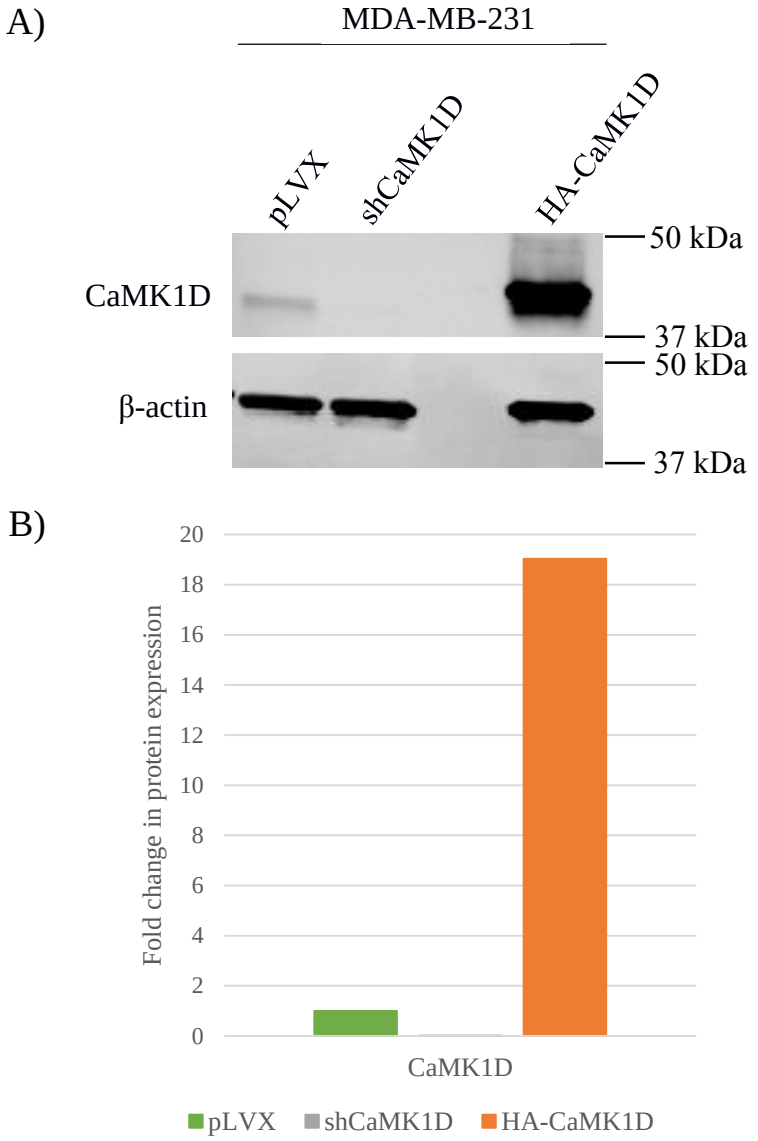

Figure 8. Western blot analysis (A) and quantification (B) of CaMK1D protein in the lentiviral-transformed MDA-MB-231 cell lines at steady state conditions. (n=1). Stable transfection of shRNA against CaMK1D effectively downregulated CaMK1D expression in MDA-MB-231 cells. The stable transfection of HA-CaMK1D resulted in a 19-fold increase in CaMK1D expression compared to the basal levels of CaMK1D expressed in MDA-MB-231, as shown by the pLVX empty vector control.

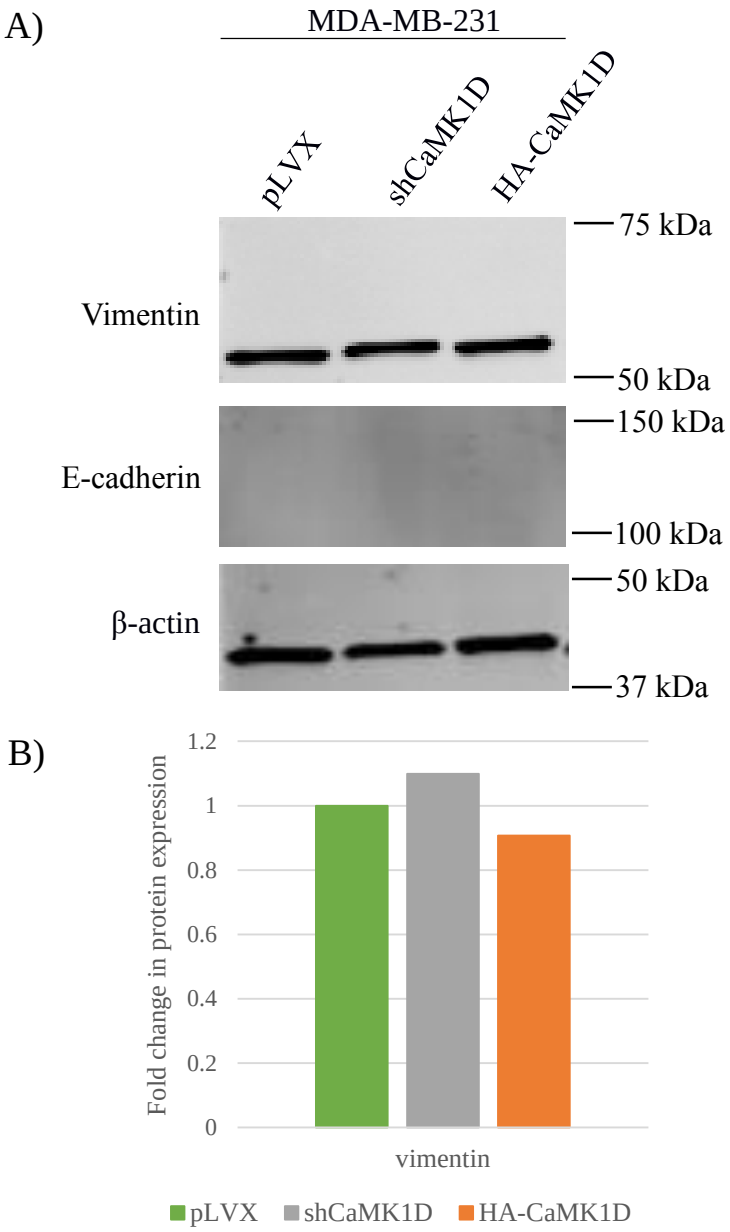

Figure 9. Western blot analyses (A) and quantification (B) of vimentin and E-cadherin proteins in the lentiviral-transformed MDA-MB-231 cell lines at steady state conditions. (n=1). No significant changes were observed in vimentin or E-cadherin expression upon CaMK1D knockdown (shCaMK1D) and overexpression (HA-CaMK1D) compared to the basal levels expressed by the empty vector (pLVX).

The MAPK/ERK pathway has been reported to be implicated in BLBCs (Toft and Cryns, 2011). Studies have shown that EGFRs are generally overexpressed in BLBCs, which subsequently promotes cell proliferation via the MAPK/ERK pathway (Hoeflich et al., 2009). Additionally, MDA-MB-231 cells have been reported to have inherent BRAF and KRAS mutations (Lehmann et al., 2011). KRAS, a GTPase and oncogene, propagates signals from proteins like c-Raf, thereby affecting cell proliferation. Western blot analyses were performed to delineate the potential association between expression levels of CaMK1D and proteins involved in the MAPK/ERK pathway (Figure 10 and 11). There was an approximate 2-fold increase in transmembrane EGFR protein upon the overexpression and knockdown of CaMK1D. No significant differences were observed in c-Raf protein levels between the empty vector and CaMK1D knockdown whereas there was a 2.5-fold decrease between CaMK1D overexpression and the empty vector. Interestingly, there was a 2.5-fold increase in MEK1/2 protein levels with CaMK1D knockdown and a 1.2-fold decrease with CaMK1D overexpression compared to basal levels of expression. The ERK1/2 protein expression followed a similar pattern with a 1.6-fold increase upon CaMK1D knockdown and a 1.2-fold decrease with CaMK1D overexpression compared to the basal level of ERK1/2 expression. Similar to c-Raf expression level, the total p38 MAPK levels did not vary between the empty vector and knockdown cell line, however, there was a 2.7-fold decrease with CaMK1D overexpression. Collectively, this data suggests the CaMK1D directly or indirectly affect members of the MAPK pathway and could intersect this pathway at several stages. Additionally, MEK1/2 and ERK1/2 could serve as a biomarker since their expression levels inversely correlate to CaMK1D expression levels.

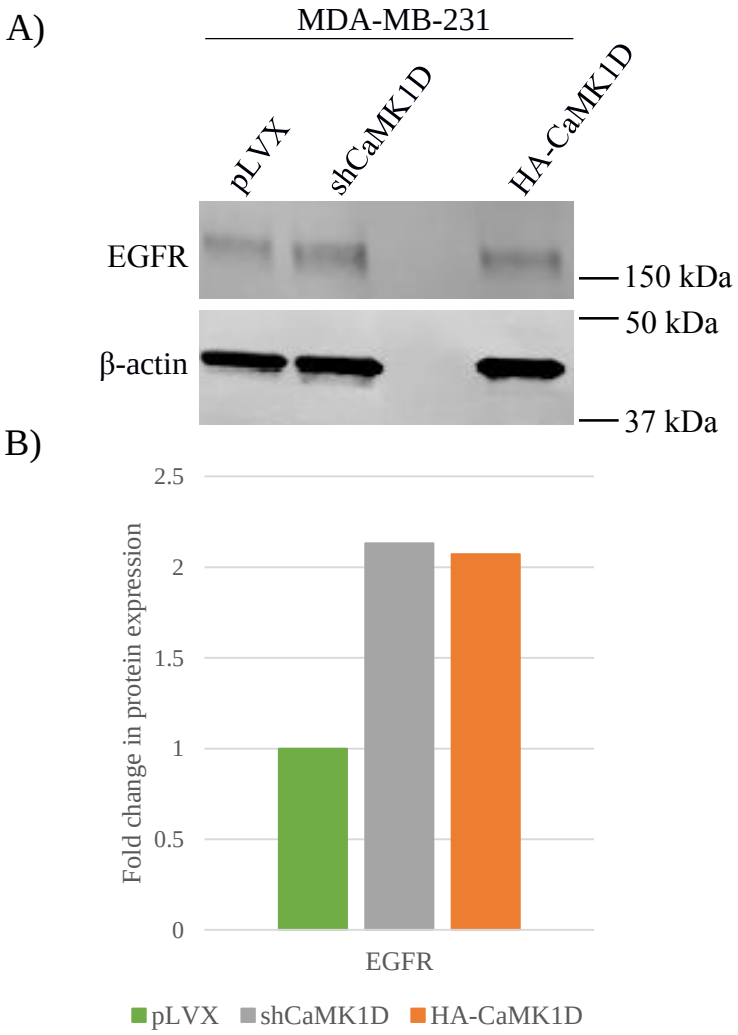

Figure 10. Western blot analysis (A) and quantification (B) of EGFR protein in the lentiviral transfected MDA-MB-231 cell lines at steady state conditions. (n=1). A 2-fold increase in EGFR expression was observed in CaMK1D knockdown and overexpression compared to the empty vector pLVX.

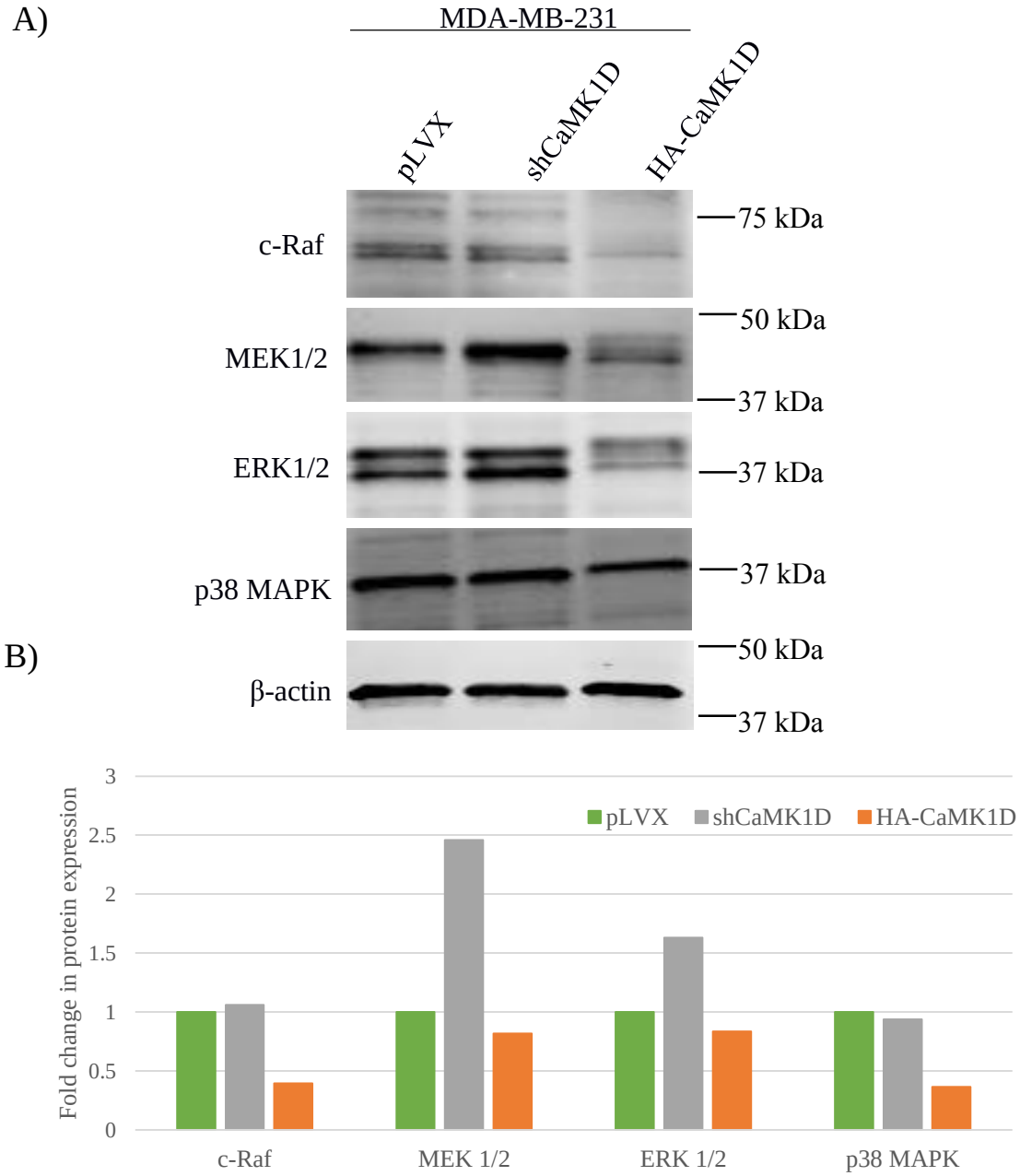

Figure 11. Western blot analyses (A) and quantification (B) of selected members of the MAPK pathway in the lentiviral transfected MDA-MB-231 cell lines at steady state conditions. (n=1) MEK1/2 and ERK1/2 show similar patterns with increased expression levels in CaMK1D knockdown cells and decreased expression upon CaMK1D overexpression. CaMK1D overexpression resulted in an approximate 2-fold decrease in c-Raf and p38 MAPK expression.

For comparison the levels of another protein, syntenin-1, which is associated with poor outcome in TNBC patients (Yang et al., 2013) was also tested. Syntenin-1 is a scaffold adaptor protein, which is known to mediate signalling from transmembrane proteins (e.g. syndecans) to cytoskeletal proteins and downstream cytosolic effectors (Sala-Valdés et al., 2012), thereby affecting cell-cell adhesion and protein transport. Since CaMK1D is a Ser/Thr kinase and syntenin-1 has known Ser phosphorylation sites, the potential correlation between CaMK1D and syntenin-1 expression levels was studied by western blot experiments (Figure 12). The overall levels of syntenin-1 increased when CaMK1D was suppressed and vice versa was observed when CaMK1D was overexpressed. Similar patterns were observed with "in-house" generated antibodies that recognise phosphorylated forms of syntenin-1. CaMK1D overexpression and knockdown resulted in a 3-fold decrease and increase, respectively, of overall syntenin-1 expression. There was an approximate 1.65-fold increase in phosphorylated Ser6, Tyr4 and Tyr47 residues of syntenin-1 upon CaMK1D knockdown. In contrast, CaMK1D overexpression led to a 3-fold, 1.3-fold, and 1.4-fold decrease in the phosphorylated syntenin-1 residues Ser6, Tyr4 and Tyr47, respectively. The decrease in phosphorylation proposes that CaMK1D overexpression downregulates syntenin-1 activity.

Due to its substrate specificity, CaMK1D would be expected to phosphorylate the Ser residues but not the Tyr residues, at least directly. However, studies suggest that these Tyr residues could be phosphorylated by members of the Src family (Sala-Valdés et al., 2012). Altogether, this data suggests that CaMK1D directly or indirectly affects syntenin-1 protein levels and activity at steady state conditions. Not only could syntenin-1 be a potential biomarker for CaMK1D inhibition in cell-based assays, this data suggests that targeting CaMK1D alone may potentially

be insufficient for treating basal-like or triple negative breast cancer as elevated syntenin expression is associated with poor prognosis. Thus, this initial result represents a potentially important link between two pathways but requires further exploration.

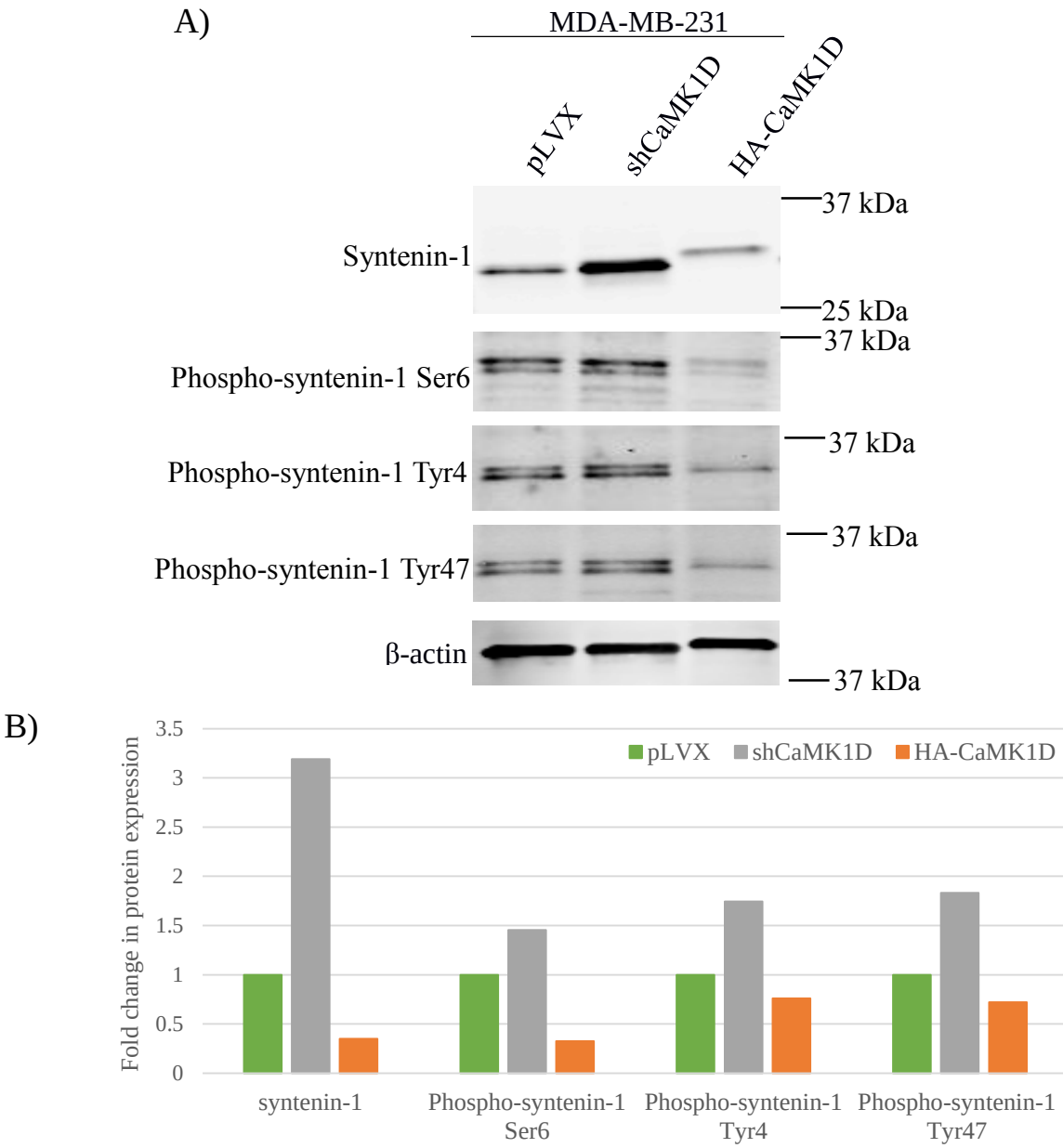

Figure 12. Western blot analyses (A) and quantification (B) of syntenin-1 and phosphorylated residues on syntenin-1 in the lentiviral transfected MDA-MB-231 cell lines at steady state conditions. (n=1). CaMK1D knockdown and overexpression resulted in a 3-fold increase and decrease in syntenin-1, respectively, compared to the pLVX control. Similarly, expression of phosphorylated Ser6, Tyr4 and Tyr47 on syntenin-1 displayed an inverse correlation to CaMK1D expression.

One of the proposed downstream nuclear targets of CaMK1D is CREB (Bergamaschi et al, 2008), a ubiquitous transcription factor that is stimulated by several pathways (Shaywitz and Greenberg, 1999). Western blot analysis of whole cell lyastes showed that there was an approximate 2-fold decrease in phosphorylated CREB in both CaMK1D knockdown and overexpression compared to the empty vector (Figure 13). CREB phosporylation could be tightly controlled by CaMK1D wherein the under- or over- expression of CaMK1D could result in the activation of different phosphatases, such as PTEN (Ross and Gericke, 2009). Subsequently, this may lead to a lower expression of phosphorylated CREB.

Detection of other potential downstream effectors of CaMK1D was achieved by analysing western blots against antibodies that target phosphorylated Ser and Thr residues (Figure 14). Three bands were observed in the phosphorylated Ser blot, referred to as Band 1 (observed between 37 and 50 kDa), Band 2 (observed between 37 and 50 kDa below Band 1) and Band 3 (just below 37 kDa). CaMK1D knockdown and overexpression resulted in a 1.2-fold increase and a 1.4-fold decrease, respectively, in Band 1 of phosphorylated Ser. There was no change between the empty vector and CaMK1D knockdown in Band 2 of phospho-Ser whilst CaMK1D overexpression showed approximately 1.1-fold decrease. CaMK1D knockdown displayed an approximate 1.3-fold increase whereas CaMK1D overexpression resulted in a 1.8-fold decrease compared to the empty vector in Band 3 of phospho-Ser. A band close to 37 kDa was also observed with the phospho-Thr antibody. Compared to the empty vector, a 1.1-fold increase and a 3.1-fold decrease in phospho Thr levels was observed in CaMK1D knockdown and overexpression respectively. Overall, the expression of proteins with phosphorylated Ser and Thr residues signifcantly decreased with CaMK1D overexpression. Hence, another kinase might be

resposible for the phosphorylation of these proteins and increased CaMK1D expression could be inhibitory for this phosphorylation. Nonetheless, quatification of the western blots suggest that the extent of the phosphorylation of Band 1 and Band 3 phospho-Ser and the phospho-Thr band inversely correlate with CaMK1D expression levels. Thus, these proteins could be identified by mass spectrometry and could serve as potential biomarkers.

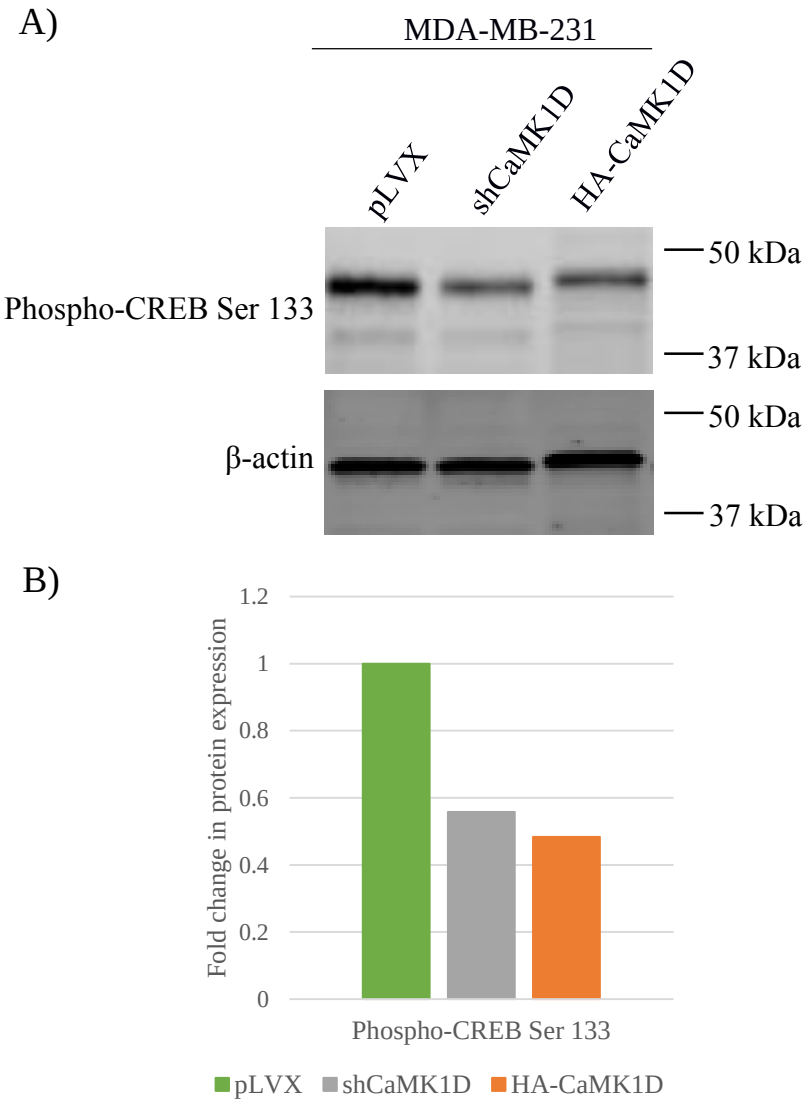

Figure 13. Western blot analysis (A) and quantification (B) of phosphorylated CREB Ser 133 in the lentiviral transfected MDA-MB-231 cell lines at steady state conditions. (n=1). There is an overall 2-fold decrease in phosphorylated Ser 133 on CREB upon CaMK1D knockdown and overexpression compared to the pLVX control.

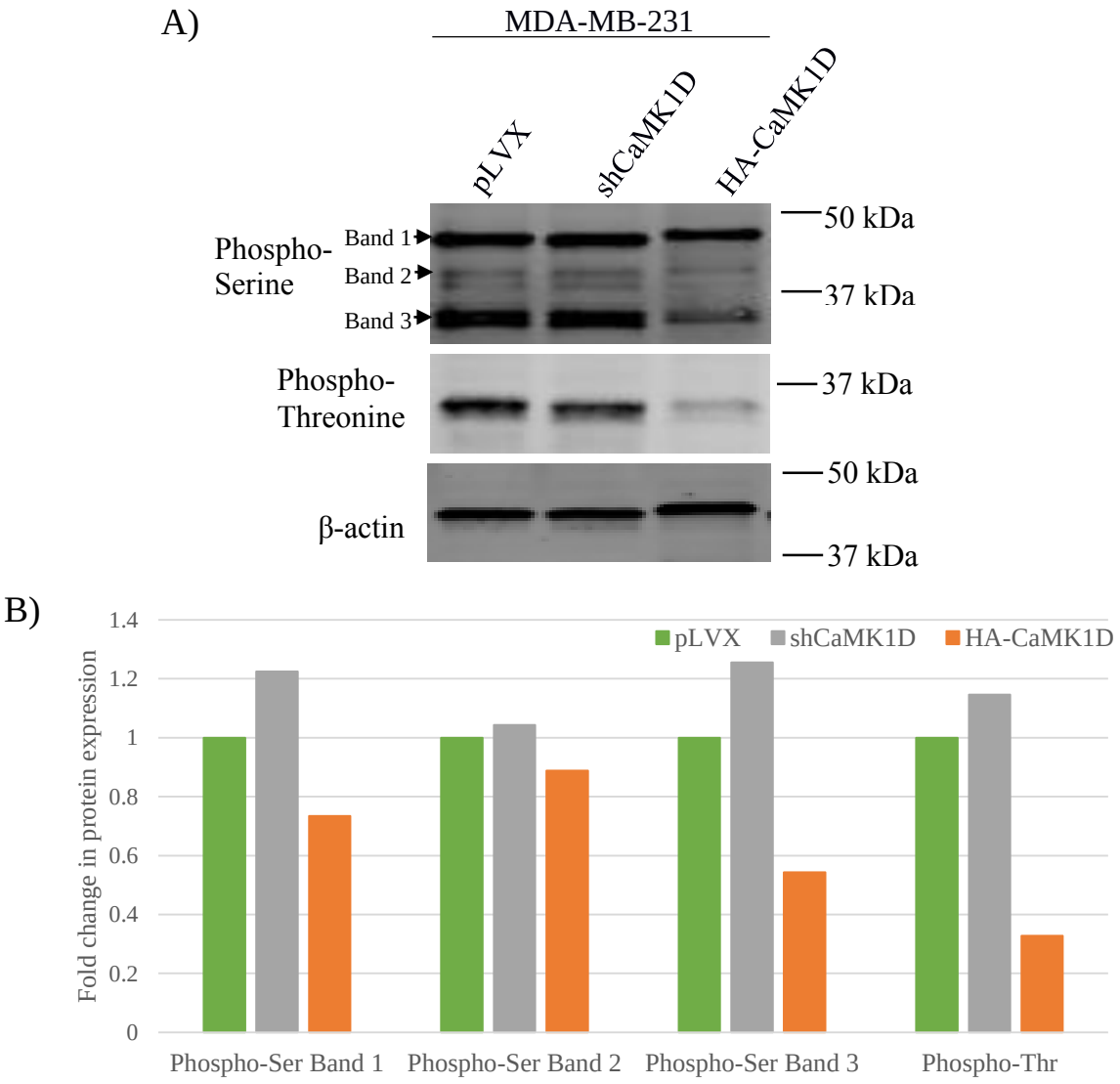

Figure 14. Western blot analyses (A) and quantification (B) of phosphorylated Serine and Threonine residues in the lentiviral transfected MDA-MB-231 cell lines at steady state conditions. (n=1). No significant change was observed with Band 2 of phosphorylated Ser. An approximate 1.2-fold increase Band 1 and Band 3 of phosphorylated Ser, and phosphorylated Thr were observed with CaMK1D knockdown. Compared to the pLVX control, CaMK1D overexpression exhibited a general 1.5- to 3 –fold decrease in phosphorylated Ser Band 1 and Band 3, and phosphorylated Thr.

4.5 Characterisation of cellular proliferation according to CaMK1D expression

The pathway involving CaMK1D is not sufficiently well understood to be able to predict whether altering the cellular CaMK1D levels affect other cell proliferation pathways. Prior to understanding the proliferative behaviour and aberrant signalling within these transformed cell lines, the seeding density was a vital parameter that had to be optimized. Thus, a cell proliferation assay was carried out on the MDA-MB-231 pLVX, shCaMK1D and HA-CaMK1D transformed cell lines at ten cell densities. A range of 7.8x10 to $4.0x10^4$ cells, each at a 2-fold density increase, were seeded in triplicates and their proliferation was studied 24 hours later (Figure 15). The readout for cell proliferation was the reduction of a fluorescent compound. This proliferation assay suggested that this range of cell density was appropriate to study the exponential growth phase of these three cell lines as the curves did not plateau. Yet, cells seeded at $4.0x10^4$ density were approximately 90-100% confluent after 24 hours of plating. Consequently, it was extrapolated that $5.0x10^3$ cells are enough to obtain an observable reading and is an appropriate cell density to use for further proliferation or cytotoxicity assays. Then to characterize the difference in proliferation across this panel of stably transfected MDA-MB-231 cells, $5.0x10^3$ cells of each transformed cell line were plated in triplicates and the proliferation was studied over 96 hours. The experiment was performed three times. (Figure 16). No significant difference was observed between the three transformed cell lines. Thus, varying CaMK1D expression levels did not affect proliferation of MDA-MB-231 cells *in vitro*.

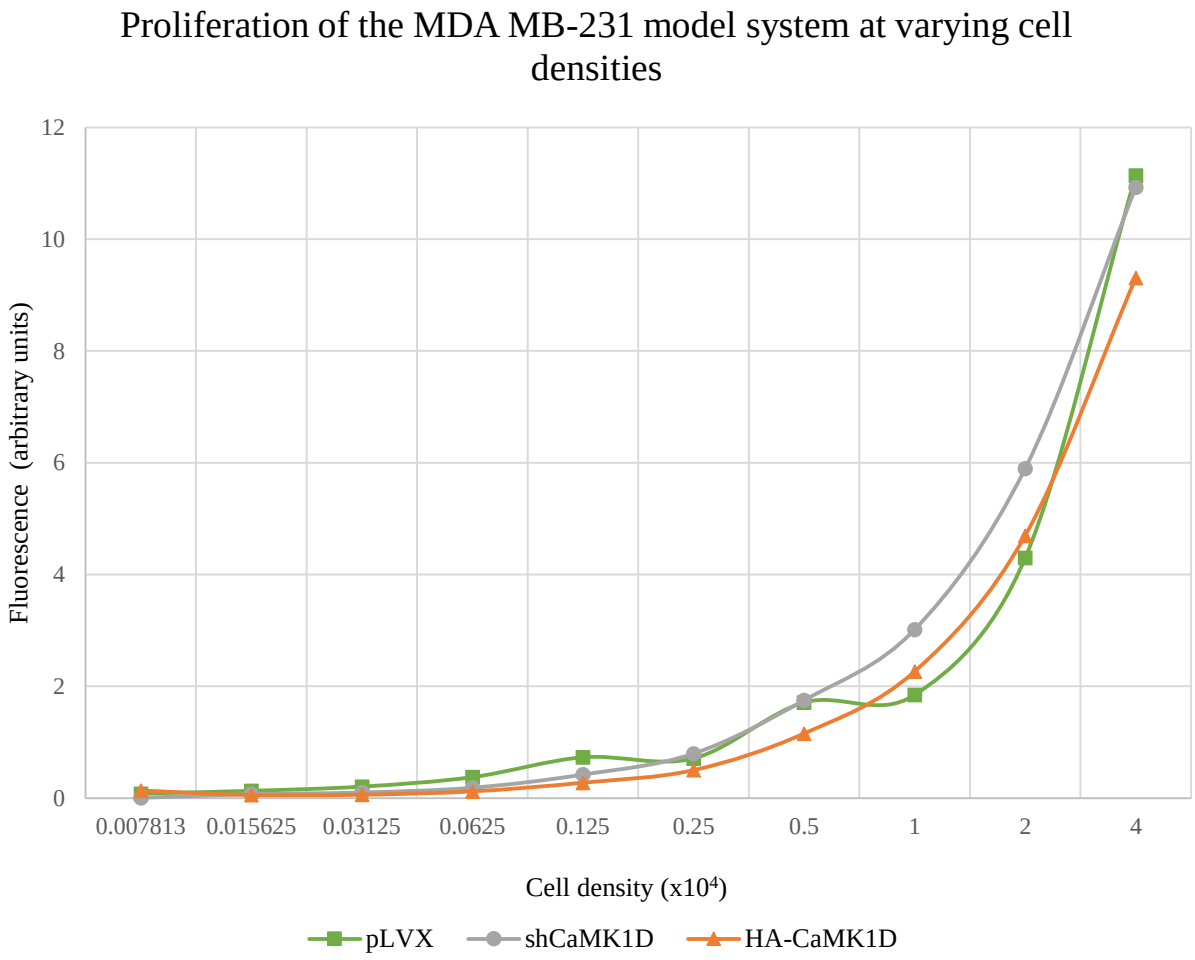

Figure 15. *In vitro* proliferation of the lentiviral transfected MDA-MB-231 cell lines at various cell densities. Cells were cultured for 24 hours in optimal serum conditions prior to the analysis of cell proliferation. Metabolically active cells reduce the reagent to a fluorescent indicator. The fluorescent signal increased exponentially from 7.8x10 to 4.0x10^4 cells in the pLVX, shCaMK1D and HA-CaMK1D transformed lines, indicating exponential growth. No significant difference was observed in the proliferation between these cell lines with varying CaMK1D expression.

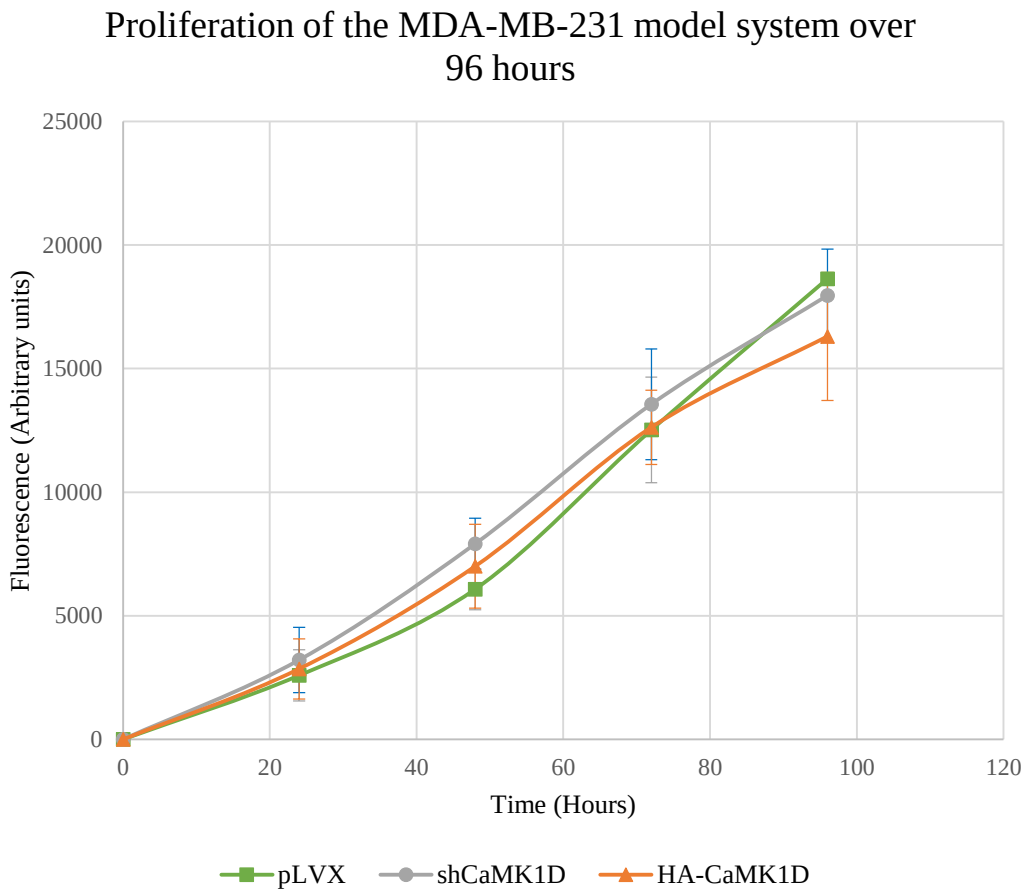

Figure 16. *In vitro* proliferation of the lentiviral transfected MDA-MB-231 cell lines analysed over 96 hours. (n=3). 5.0x10^3 cells were seeded and cultured in optimal serum conditions. Metabolically active cells reduce the reagent to a fluorescent indicator. There was a linear increase in proliferation throughout the 96 hours yet no significant difference in the proliferation was observed between these cell lines with varying CaMK1D expression. Data are means ± s.e.m.

It is possible that the lack of difference in proliferation across this panel of MDA-MB-231 transformed cell lines is due to the presence of serum-derived growth factors in the growth media, which may overshadow the effect of CaMK1D overexpression or downregulation. To investigate the proliferative effect of the CaMK1D kinase under suboptimal conditions, the proliferation of this model system was studied under four serum concentrations with an approximate 3-fold difference; serum-free, 1% serum, 3% serum and 10% serum conditions. Cells were plated in triplicates with a seeding density of $5.0x10^3$ and were studied over 96 hours (Figure 17, 18, 19). The experiment was performed three times. Within 24 hours, a reduction in cell proliferation was observed under the serum-free condition across all three cell lines. No significant difference was observed between the 1%, 3% and 10% serum conditions in all three cell lines until 48 hours after plating. At 48 hours, the pLVX and CaMK1D knockdown cells in 1% and 10% serum conditions exhibited lower proliferation than that at 3% serum condition, whereas there was no difference between these three conditions in the CaMK1D overexpressing cells. Yet at 72 hours in all three cell lines, there was no difference in proliferation between the 3% and 10% conditions whilst approximately half the proliferation was observed with cells at 1% serum. Across all three cell lines, the growth of cells at 1% FBS started to plateau at 48 hours and the proliferation of cells at 10% FBS did not plateau over the course of the assay. Interestingly, under the 3% serum condition, proliferation of cells containing the empty vector started to plateau at 72 hours whereas the proliferation of CaMK1D knockdown and overexpressing cells did not reach a plateau throughout the experiment.

Figure 17. *In vitro* proliferation of the MDA-MB-231 pLVX cell line analysed over 96 hours under various serum conditions. (n=3). Cells were seeded at a $5.0x10^3$ cell density. Metabolically active cells reduce the reagent to a fluorescent indicator. A general decrease in fluorescence was observed throughout the course of the experiment under the serum-free condition. In 1% FBS, cells grew exponentially until 48 hours, after which it reached the stationary phase. A similar pattern was observed with 3%FBS. Cells in 10% FBS continued to grow exponentially throughout the 96 hours. Data are means ± s.e.m.

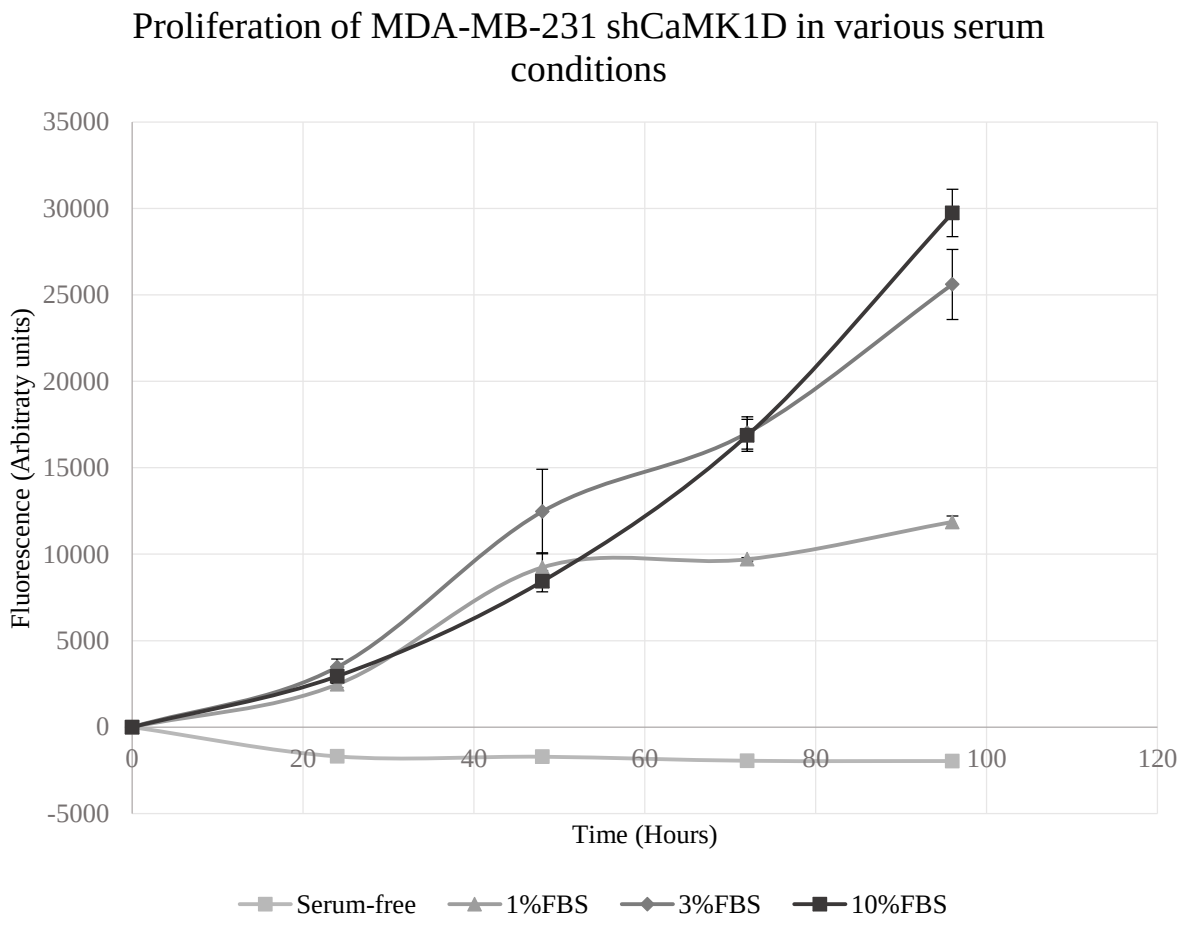

Figure 18. *In vitro* proliferation of the MDA-MB-231 shCaMK1D cell line analysed over 96 hours under various serum conditions. (n=3). Cells were seeded at a $5.0x10^3$ cell density. Metabolically active cells reduce the reagent to a fluorescent indicator. A general decrease in fluorescence was observed throughout the course of the experiment under the serum-free condition. In 1% FBS, cells grew exponentially until 48 hours, after which it reached the stationary phase. Cells in 3% and 10% FBS continued to grow linearly throughout the 96 hours. Data are means ± s.e.m.

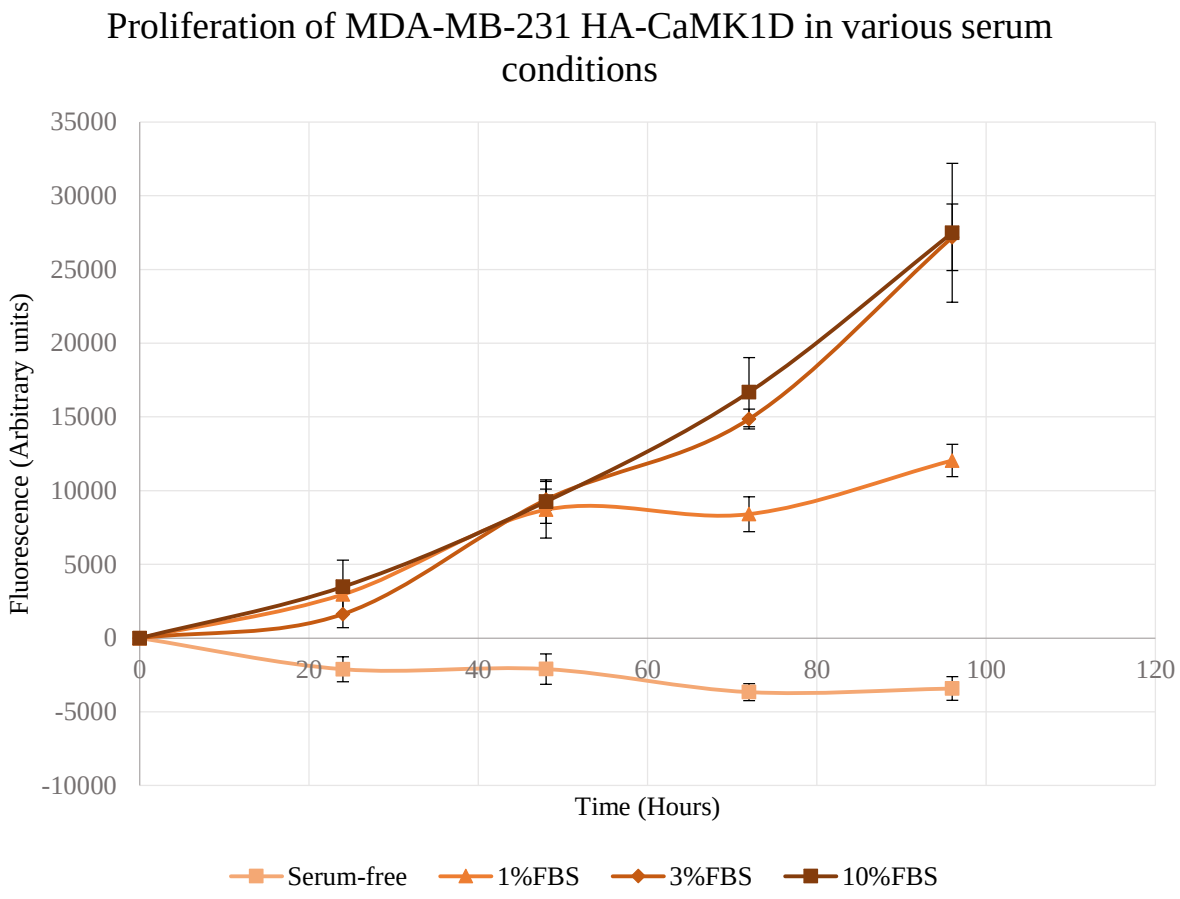

Figure 19. *In vitro* proliferation of the MDA-MB-231 HA-CaMK1D cell line analysed over 96 hours under various serum conditions. (n=3). Cells were seeded at a $5.0x10^3$ cell density. Metabolically active cells reduce the reagent to a fluorescent indicator. A general decrease in fluorescence was observed throughout the course of the experiment under the serum-free condition. In 1% FBS, cells grew exponentially until 48 hours, after which it reached the stationary phase. Cells in 3% and 10% FBS continued to grow exponentially throughout the 96 hours. Data are means ± s.e.m.

In all the three MDA-MB-231 transformed cell lines, the serum-free condition leads to about 67% reduction in overall fluorescence. Proliferation under the highly sub-optimal condition of 1% FBS was not favourable either as the cells reached the stationary phase of growth within 48 hours of the assay. Although a similar pattern of overall cell proliferation was observed under the 3% and 10% FBS conditions, statistically significant differences were observed at certain time intervals (Figure 20 and 21). Under the 3% FBS conditions, there was no statistically significant difference between the three transformed cell lines at 24 and 96 hours whereas there was no statistically significant difference at 24 and 48 hours at 10% FBS. However, a significant statistical difference was observed between CaMK1D knockdown and overexpression at 48 hours in 3% FBS when CaMK1D knockdown and overexpressing cells proliferated 1.2-fold and 1.6-fold less than the empty vector control, respectively. A similar observation is made at 72 hours, when CaMK1D knockdown and overexpressing cells proliferated 1.2-fold and 1.3-fold less compared to the pLVX control, respectively. Under the optimal 10% FBS conditions, an approximate 1.3-fold less proliferation was observed in CaMK1D knockdown and overexpression compared to the control at 72 and 96 hours. Due to the statistically significant inconsistencies observed in different serum conditions at different time points, further cytotoxicity assays were performed under the sub-optimal 3% FBS and the optimal 10% FBS conditions.

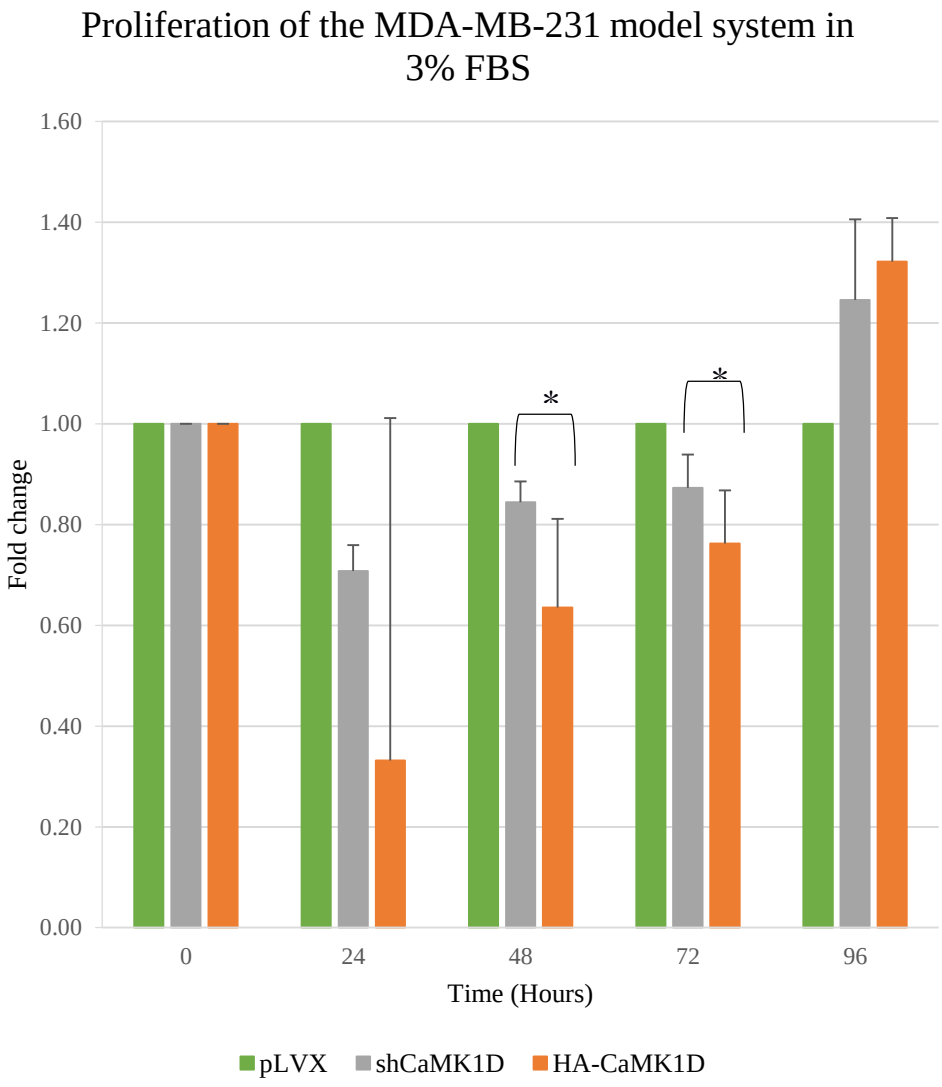

Figure 20. *In vitro* proliferation of the lentiviral transfected MDA-MB-231 cell lines analysed over 96 hours in 3%FBS. The fold changes of CaMK1D knockdown and overexpression were compared to the empty vector control. At 24, 48 and 72 hours, the fold change in CaMK1D overexpression was smaller than that observed with CaMK1D knockdown. However, at 96 hours, the fold change in CaMK1D overexpression is higher than that of CaMK1D knockdown. It should be noted that there is a significant difference in the fold change in proliferation between CaMK1D knockdown and CaMK1D overexpression at 48 and 72 hours. Asterisk indicates $P < 0.05$. Data are means ± s.e.m.

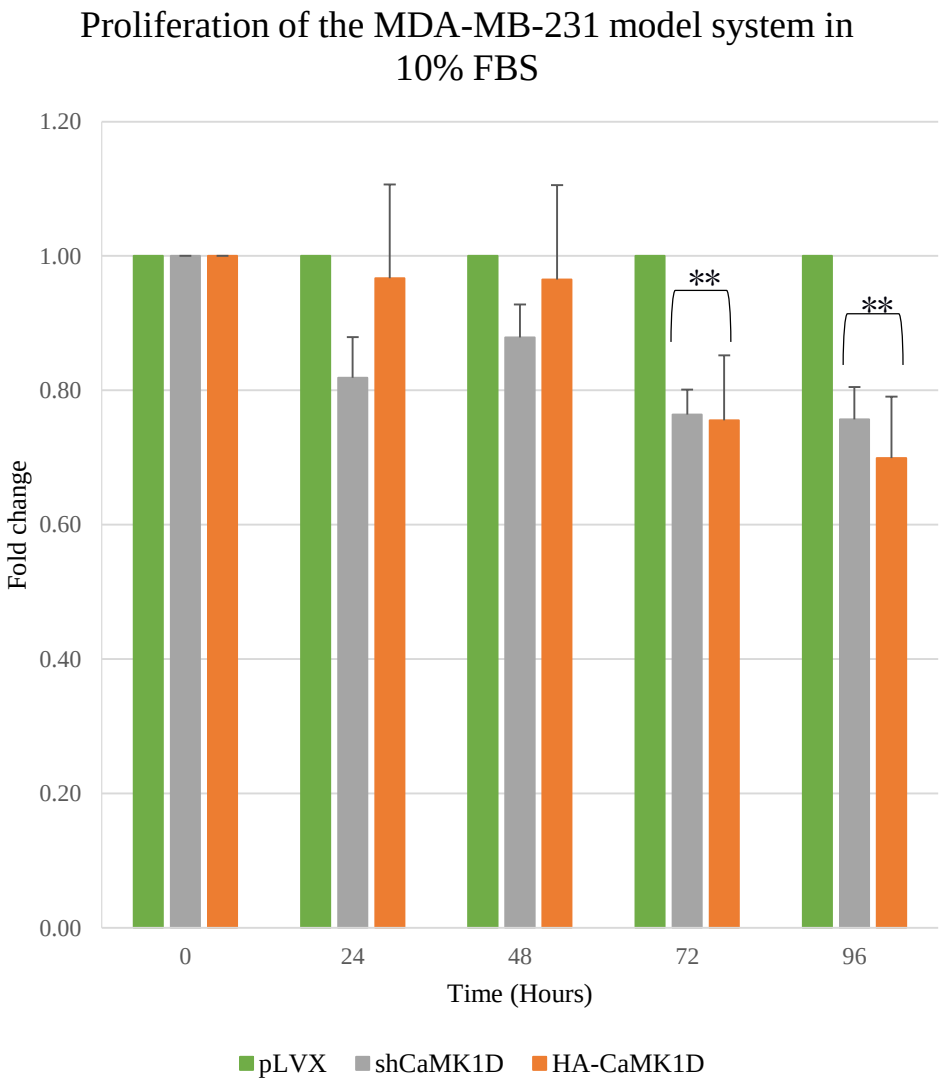

Figure 21. *In vitro* proliferation of the lentiviral transfected MDA-MB-231 cell lines analysed over 96 hours in 10%FBS. The fold changes of CaMK1D knockdown and overexpression were compared to the empty vector control. At 24 and 48 hours, the fold change in CaMK1D overexpression was higher than that observed with CaMK1D knockdown. They were similar at 72 hours, however, at 96 hours, the fold change in CaMK1D knockdown is higher than that of CaMK1D overexpression. It should be noted that there is a very significant difference in the fold change in proliferation between CaMK1D knockdown and CaMK1D overexpression at 72 and 96 hours. Double asterisk indicates $P < 0.005$. Data are means ± s.e.m.

4.6 The potency of a potential CaMK1D-specific inhibitor on cellular proliferation

Cytotoxicity assay is a vital tool for drug discovery as it acts as the preliminary readout for a drug's potency. It allows for the *in vitro* study of the toxic effects of the compound via necrosis or apoptosis on the proliferation of the cells. After the optimisation of the two parameters, cell density and serum condition, the inhibitor concentration used for cytotoxicity assays had to be optimised. Although we were unable to culture enough of the HCC70 panel of transformed cell lines for several cell-based assays, microarray data suggests that HCC70 cells have inherently higher levels of CaMK1D expression than MDA-MB-231 cells. Thus, the initial cytotoxicity assay using the proposed CaMK1D-specific GSK-3 XIII inhibitor was conducted on the HCC70 model. For this, cells were plated with a seeding density of $4.0x10^3$ cells/well in triplicates and incubated for 72 hours in media containing 10% FBS. Cells were then exposed to GSK-3 XIII at 6 different concentrations with a 10-fold difference for 48 hours prior to the proliferation reading (Figure 22, 23, 24). The half maximal inhibitory concentration (IC_{50}) value is an indicator of the drug's potency as it measures the concentration of compound required to inhibit a certain cellular process. The IC_{50} values of empty vector, CaMK1D knockdown and CaMK1D overexpression were 5.99 µM, 4.04 µM and 11.2 µM respectively. Hence, increasing levels of CaMK1D expression resulted in an increased IC_{50} value. This data suggests that the GSK-3 XIII inhibitor could be CaMK1D-specific. This data also proposes that 10 µM of GSK-3 XIII inhibitor would be suffice to observe a difference in proliferation across the panel of stably transfected cell lines in other cell-based assays.

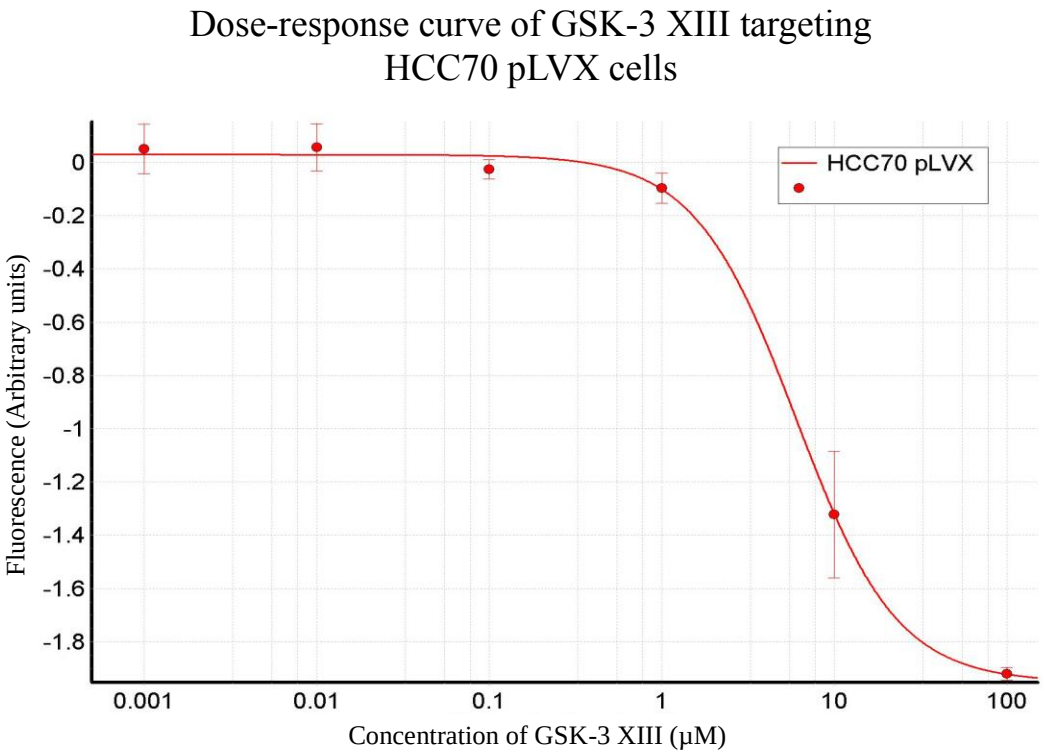

Figure 22. *In vitro* cytotoxicity assay of GSK3 XIII on the lentiviral transfected HCC70 pLVX cells. Cells were cultured for 48 hours in optimal serum conditions prior to the analysis of cell proliferation. Cells were tested at inhibitor concentrations, ranging from 0.001 to 100 µM, each with a 10-fold difference. Metabolically active cells reduce the tetrazolium reagent to a fluorescent indicator. The IC_{50} value of this inhibitor in HCC70 cells expressing basal level of CaMK1D was 5.99 µM.

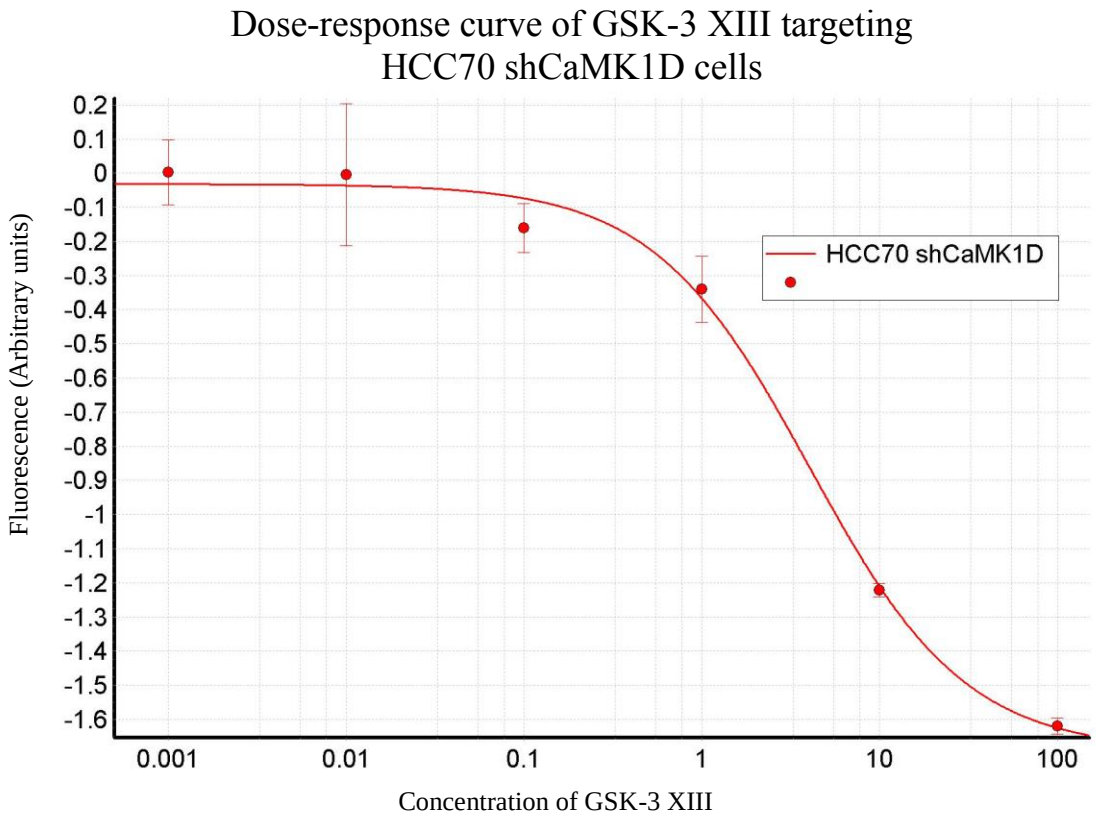

Figure 23. ***In vitro*** **cytotoxicity assay of GSK3 XIII on the lentiviral transfected HCC70 shCaMK1D cells.** Cells were cultured for 48 hours in optimal serum conditions prior to the analysis of cell proliferation. Cells were tested at inhibitor concentrations, ranging from 0.001 to 100 µM, each with a 10-fold difference. Metabolically active cells reduce the tetrazolium reagent to a fluorescent indicator. The IC_{50} value of this inhibitor in HCC70 cells expressing no/low levels of CaMK1D, was 4.04 µM.

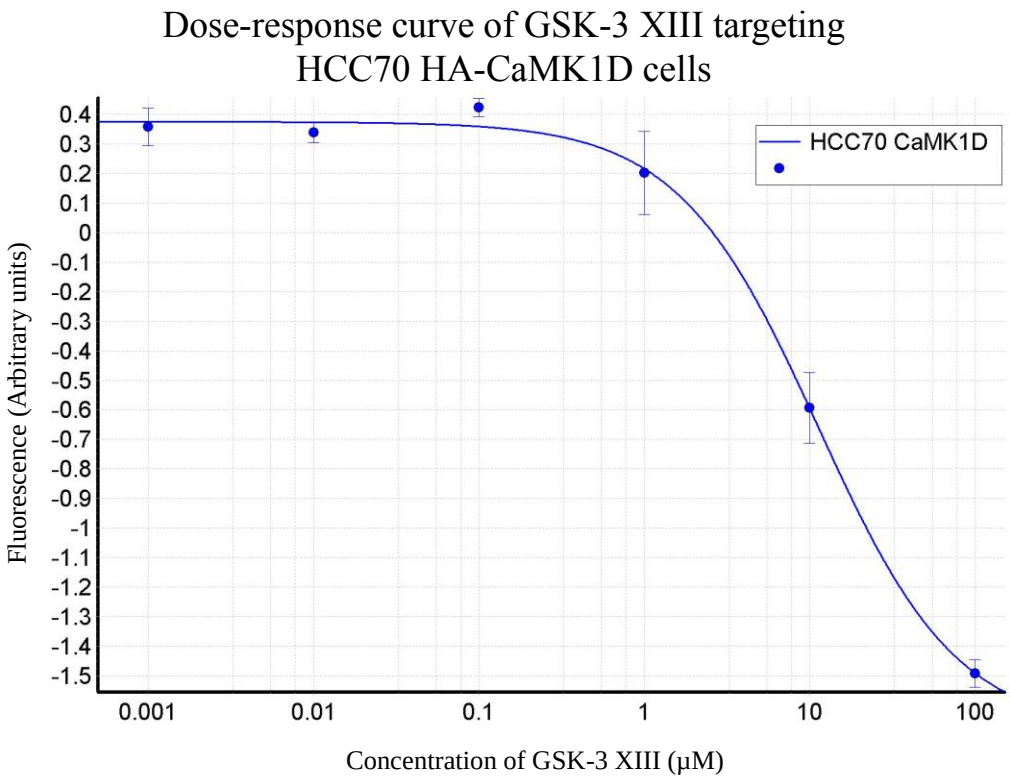

Figure 24. ***In vitro*** **cytotoxicity assay of GSK3 XIII on the lentiviral transfected HCC70 HA-CaMK1D cells.** Cells were cultured for 48 hours in optimal serum conditions prior to the analysis of cell proliferation. Cells were tested at inhibitor concentrations, ranging from 0.001 to 100 µM, each with a 10-fold difference. Metabolically active cells reduce the tetrazolium reagent to a fluorescent indicator. The IC_{50} value of this inhibitor in HCC70 cells overexpressing CaMK1D was 11.2 µM.

.

Cytotoxicity assays using 10μM of GSK-3 XIII inhibitor were then performed on the panel of MDA-MB-231 transformed cell lines in 3% FBS and 10% FBS conditions. Most inhibitors are insoluble in water, thus DMSO is used to reconstitute the inhibitors. To eliminate the effects of DMSO on cellular behaviour, experiments were carried out with 1% DMSO controls. Cells were seeded at $5.0x10^3$ cells/well density in triplicates and the experiment was performed three times. The experiment was carried out for 144 hours ensure that the effects of CaMK1D are not latent (Figure 25-28). Although GSK-3 XIII is a known ATP-analogue, its suggested affinity for CaMK1D proposes that the CaMK1D overexpressing cells would be preferentially targeted over the CaMK1D knockdown cells. However, no significant difference was observed between the three cell lines. Throughout the course of the experiment, CaMK1D knockdown resulted in a higher fold change than CaMK1D overexpression compared to the empty vector. Additionally, at 24 hours, a higher proliferation was observed with CaMK1D overexpressing cells than the empty vector and CaMK1D knockdown cells in the 3% and 10% FBS conditions. The differences between the three cell lines were negligible because the data was statistically insignificant. However, after 24 hours, the three transformed cell lines followed a similar pattern of decrease in cell viability, which could be the result of cell death or cytostasis. Since a decrease in cell proliferation was observed in all three transformed cell lines under both conditions, the inhibitor targeted a protein involved in cell proliferation. This suggests that the effect was not CaMK1D-specific, as expected, given its relatively broad kinase specificity.

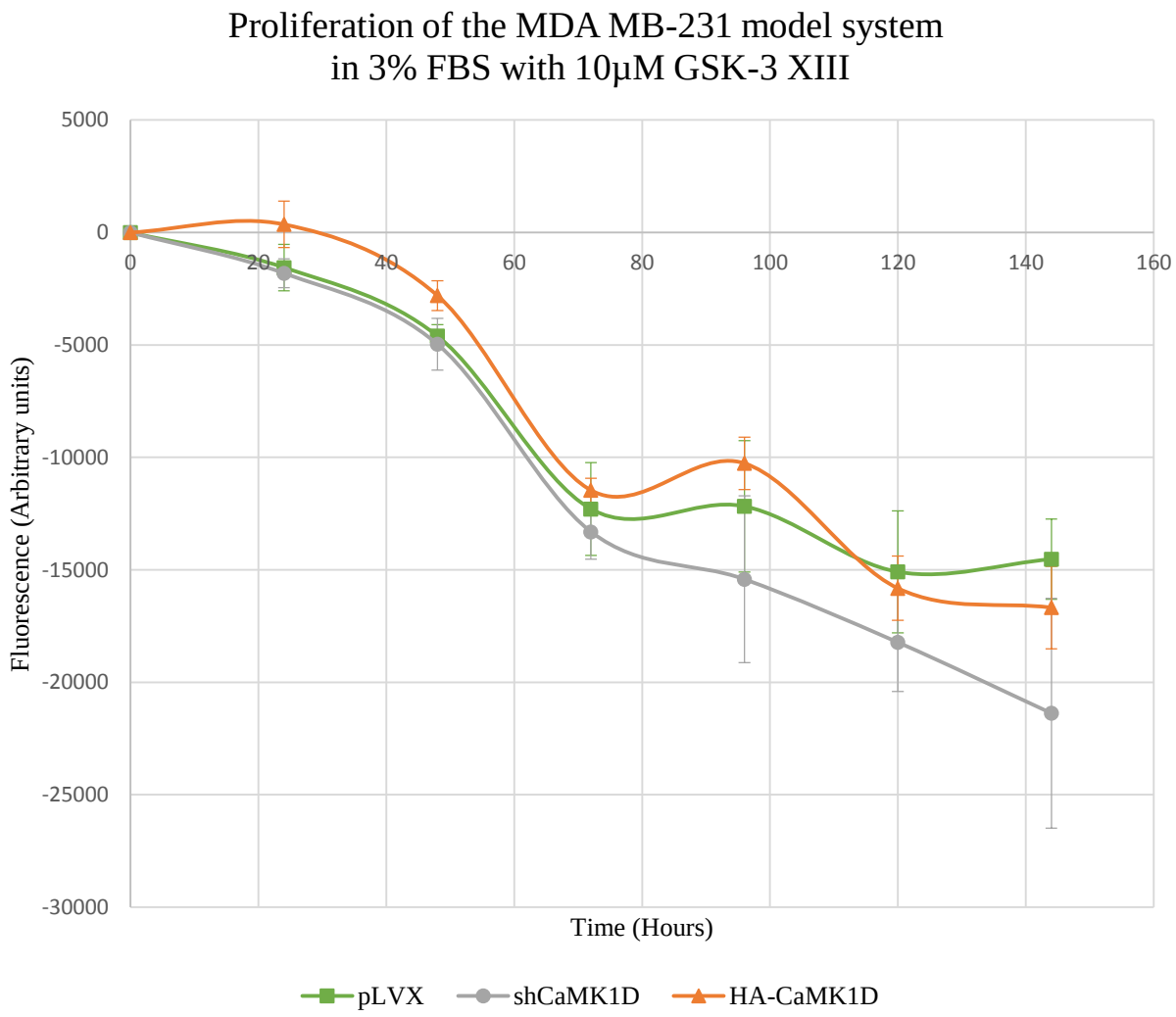

Figure 25. ***In vitro*** **cytotoxicity profile of GSK-3 XIII on the lentiviral transfected MDA-MB-231 cell lines in 3% FBS.** Cells were seeded at a $5.0x10^3$ cell density. Metabolically active cells reduce the tetrazolium reagent to a fluorescent indicator. The three cell lines follow a similar pattern of reduced cell viability until 72 hours. There is a slight increase in cell proliferation in CaMK1D overexpression and pLVX at 96 hours compared to CaMK1D knockdown cells. The reduction in cell viability continues in all three cell lines until 144 hours. Data are means ± s.e.m.

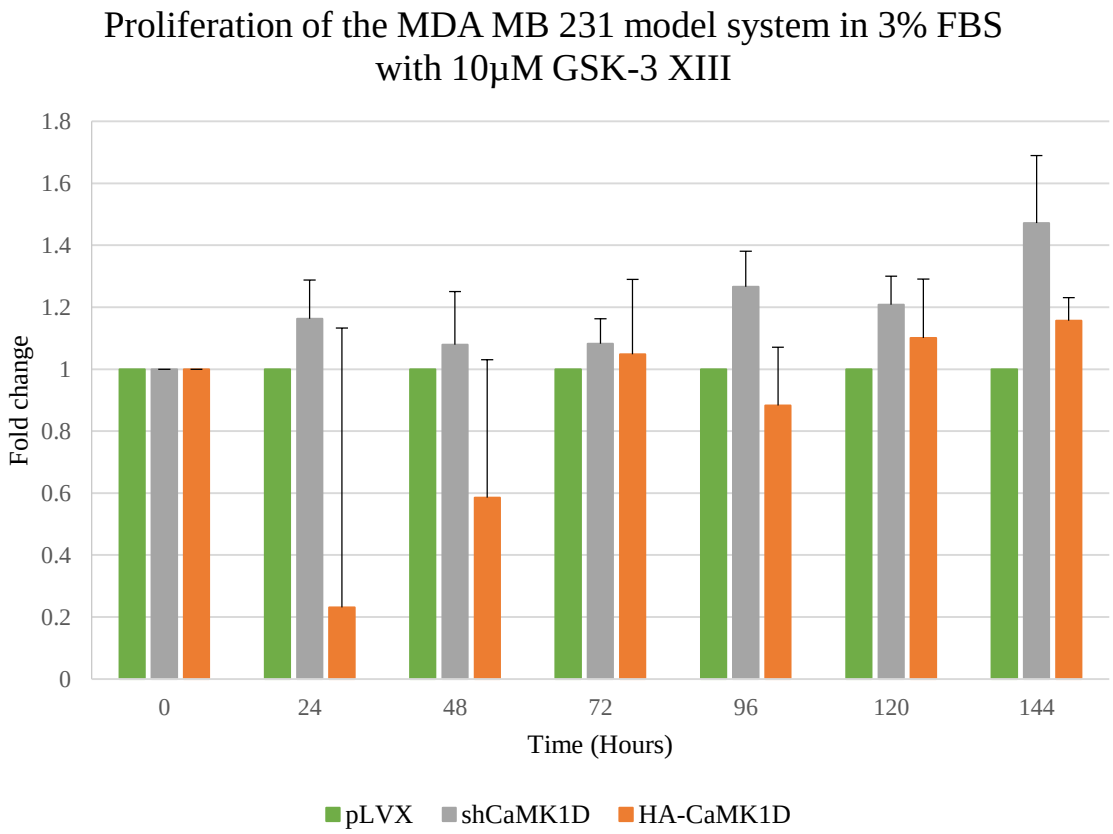

Figure 26. *In vitro* cytotoxicity profile of GSK-3 XIII on the lentiviral transfected MDA-MB-231 cell lines in 3% FBS. Overall, the fold change was greater between the CaMK1D knockdown and control cells compared to those observed between the CaMK1D overexpressing and control cells. However, the data was not statsititcally significant. Data are means ± s.e.m.

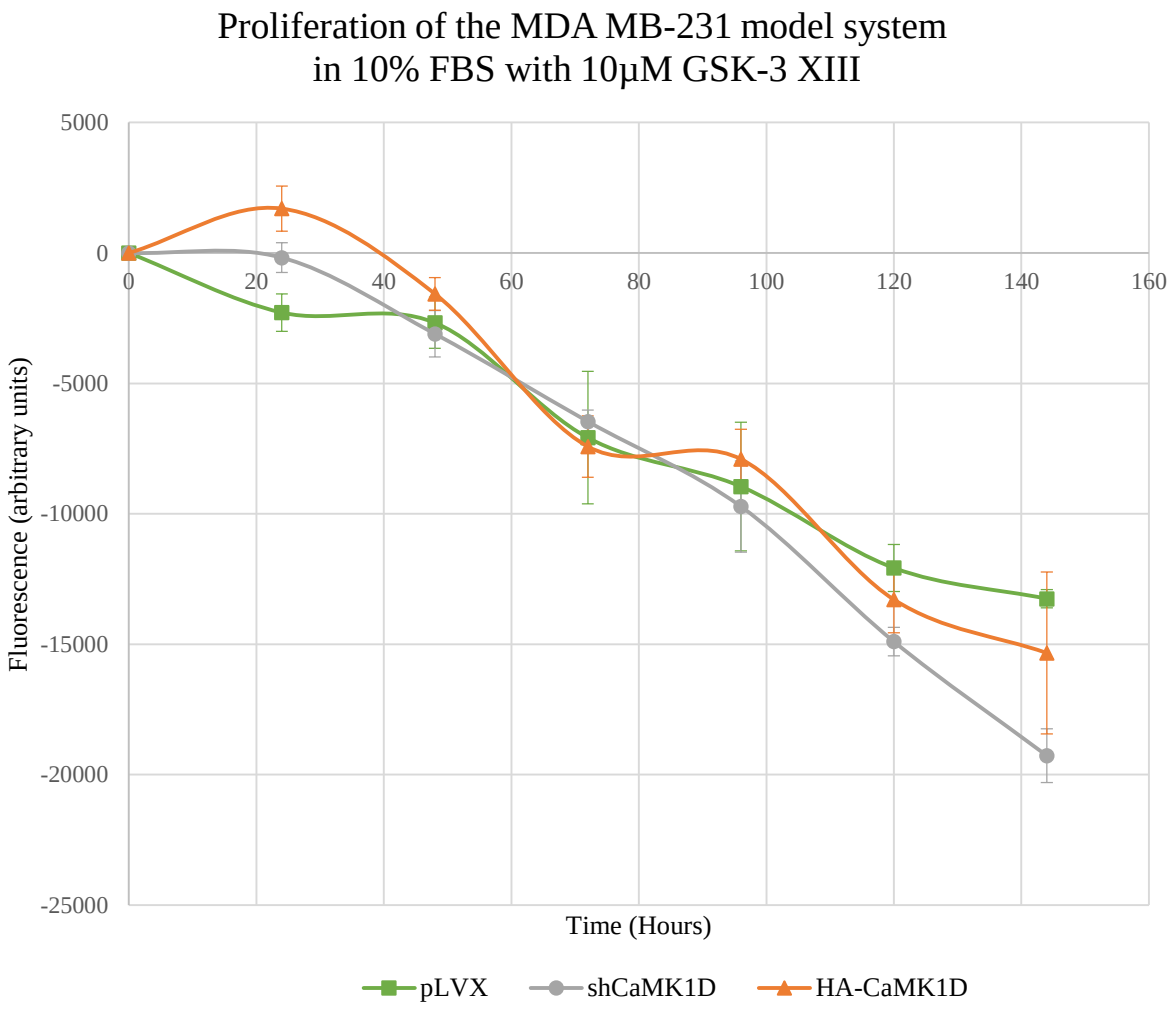

Figure 27. *In vitro* cytotoxicity profile of GSK3 XIII inhibitor on the lentiviral transfected MDA-MB-231 cell lines in 10% FBS. Cells were seeded at a $5.0x10^3$ cell density. Metabolically active cells reduce the tetrazolium reagent to a fluorescent indicator. Although CaMK1D overexpression exhibited a slight increase in cell proliferation at 24 and 96 hours compared to the control and CaMK1D knockdown cells, the three cell lines followed a similar pattern of reduction in cell viability until 144 hours. Data are means ± s.e.m.

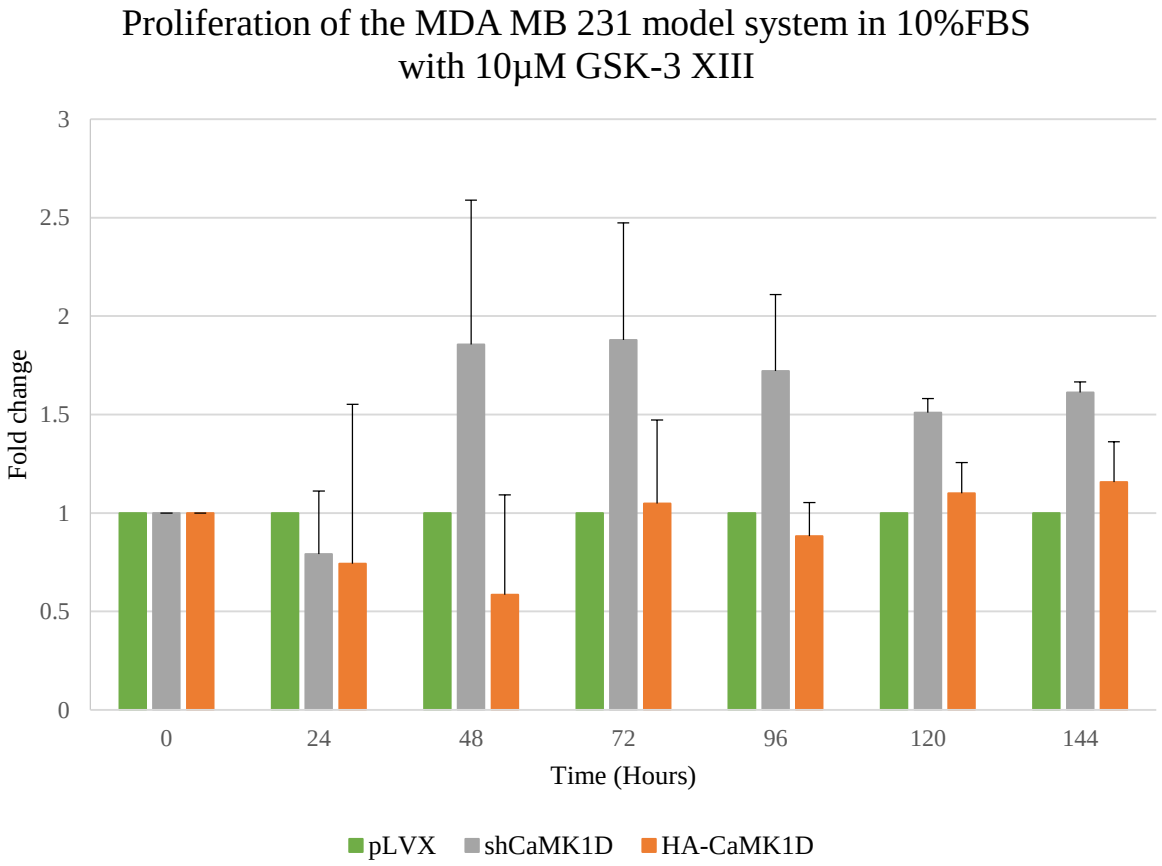

Figure 28. ***In vitro*** **cytotoxicity profile of GSK3 XIII inhibitor on the lentiviral transfected MDA-MB-231 cell lines in 10% FBS**. Overall, the fold change was greater between the CaMK1D knockdown and control cells compared to those observed between the CaMK1D overexpressing and control cells. However, the data was not statsititcally significant. Data are means ± s.e.m.

4.7 The potency of a potential CaMK1D-specific inhibitor on cell migration

It has been reported that CaMK1D overexpression results in increased cell migration, a characteristic of EMT. Scratch wound assays were performed to determine if GSK-3 XIII targets a migration pathway associated with the level of CaMK1D expression. For preliminary investigation, cells of the MDA-MB-231 panel were cultured in optimal serum conditions, i.e.10% FBS, and were seeded at a $2.1x10^4$ cell density into each chamber of Ibidi's culture-inserts. These inserts were lifted off after the cells attained 90% -100% confluency, which was 48 hours after seeding. Cells were then cultured in media containing 10µM of GSK-3 XIII and the controls were cultured in 1% DMSO (Figure 29 and 30). MDA-MB-231 pLVX and shCaMK1D under the control conditions closed the gap after 24 hours. Although the MDA-MB-231 CaMK1D cells in 1% DMSO did not close the gap completely after 24 hours, the gap was narrower. This difference could be due to the result of pipetting error when plating the cells, resulting in fewer cells being plated in the insert. Nonetheless, all three cell lines did not close the gap after 24 hours of inhibition by GSK-3 XIII. Since the inhibitors effect was not limited by the varying CaMK1D levels expressed by this model system, this migration assay further indicates that GSK-3 XIII probably targets pathways involved in proliferation and migration that are largely independent of CaMK1D.

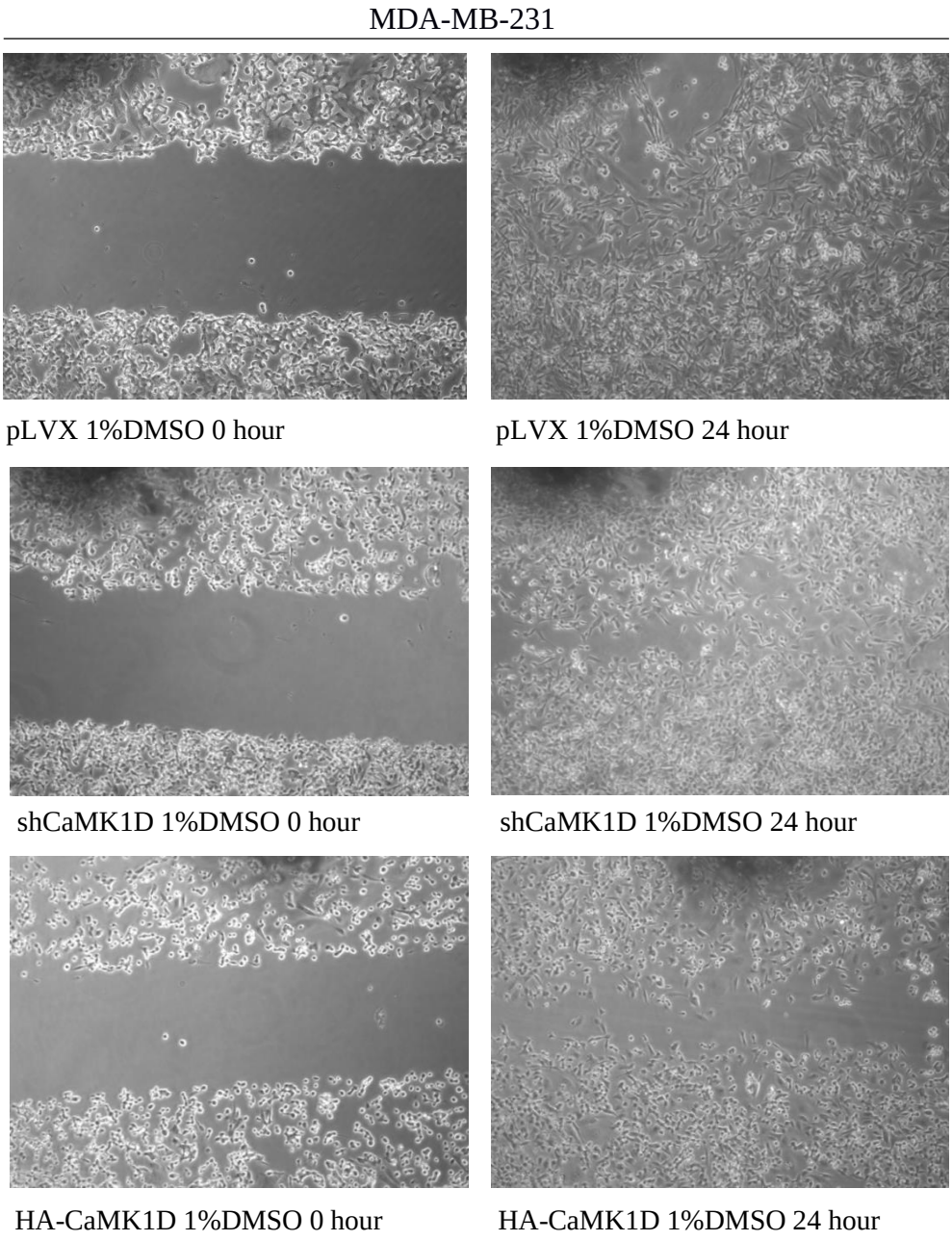

Figure 29. Scratch-wound assay of the MDA-MB-231 model system in 1% DMSO, imaged at 10X magnification. Cells were seeded at $2.1x10^4$ density in optimal serum conditions. pLVX- and shCaMK1D- expressing cells closed the gap completely after 24 hours whereas the gap was almost closed yet incompletely with CaMK1D overexpressing cells.

MDA-MB-231

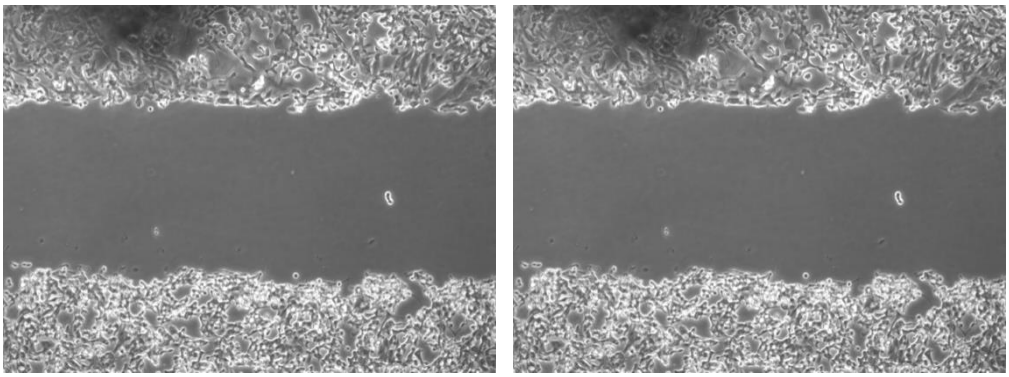

pLVX 10µM GSK-3 XIII 0 hour pLVX 10µM GSK-3 XIII 24 hour

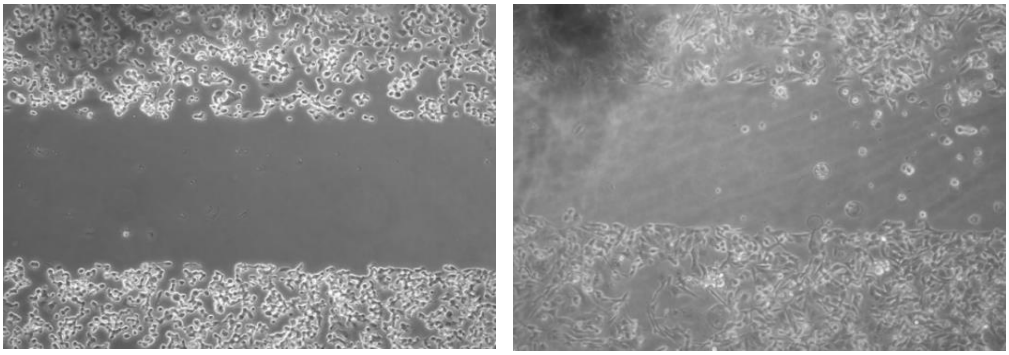

shCaMK1D 10µM GSK-3 XIII 0 hour shCaMK1D 10µM GSK-3 XIII 24 hour

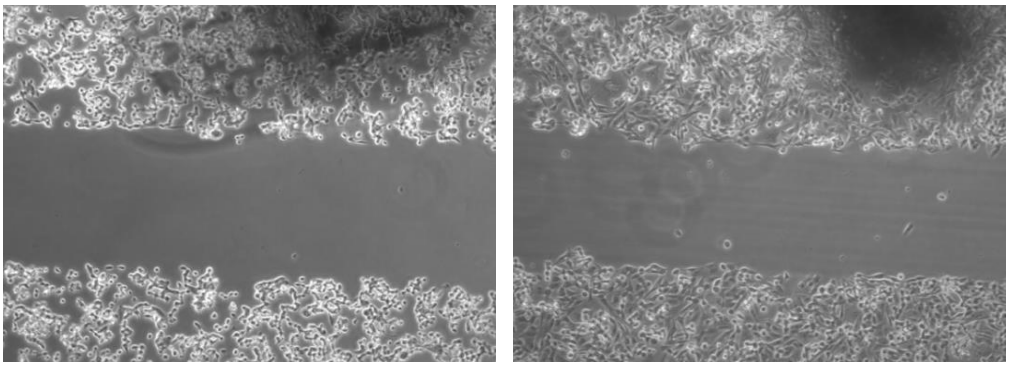

HA-CaMK1D 10µM GSK-3 XIII 0 hour HA-CaMK1D 10µM GSK-3 XIII 24 hour

Figure 30. Scratch-wound assay of the MDA-MB-231 model system in 10µM GSK-3 XIII substituted in 1% DMSO, imaged at 10X magnification. Cells were seeded at $2.1x10^4$ density in optimal serum conditions. The gap did not close after 24 hours in the three stably transfected cell lines.

4.8 Morphology of the MDA-MB-231 model system in a more physiological environment

No significant difference in cellular proliferation or migration was observed with the exposure of the GSK-3 XIII inhibitor to the MDA MB-231 model system. However, these cell-based assays were conducted on 2D cultures, which do not mimic a physiological environment. Since these transformed cell lines displayed morphological differences in 2D culture, we were interested to see if morphological differences across these cell lines were still observable in a 3D culture. To study this, these transformed cell lines were plated onto matrigel, a gelatinous protein matrix that shares similarities with the basement membrane and therefore partially resembles a physiological environment (Figure 31). The vector control grew in colonies that were rounded; cells with this morphological feature tend to have robust cell-cell adhesion (Kenny et al., 2007). Cells overexpressing CaMK1D displayed the same morphological feature however these colonies of cell aggregates appeared to be larger compared to the empty vector control. The CaMK1D knockdown cells grew with a stellate morphology exhibiting more protrusions. CaMK1D knockdown cells appear to form less cohesive cell interactions in contrast to the pLVX control and CaMK1D overexpression cell lines. Further staining, for example, of the nucleus or cell membrane proteins, could be performed to characterise these morphological differences.

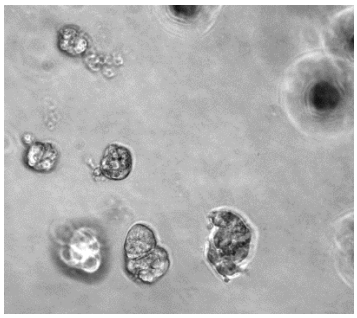

MDA-MB-231 pLVX

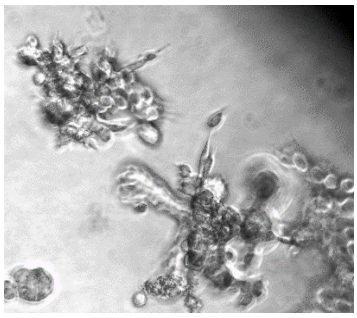

MDA-MB-231 shCaMK1D

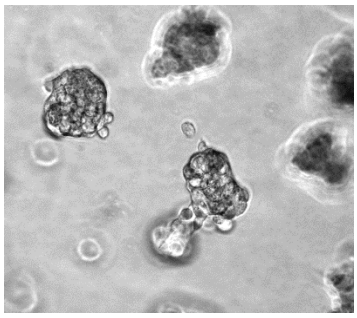

MDA-MB-231 HA-CaMK1D

Figure 31. Morphology of MDA-MB-231 model system in 3D culture, viewed at 10X magnification. Cells were seeded at $1.0x10^4$ density under optimal serum conditions in matrigel. Cell expressing empty vector (left) grew in round colonies. Similar morphology was observed with CaMK1D overexpression (right) but the aggregates appeared to be larger. CaMK1D knockdown (middle) resulted in cells protruding from the colony.

5. Discussion

There is an unmet clinical need for effective treatment of TNBC and BLBC, and the design mechanism-based small molecule therapeutic agents is a viable route for meeting this need. The first-line treatment for patients with TNBC generally involves a non-specific chemotherapeutic regime, which is generally linked with poor long-term outcomes and off-target effects (Rakha et al., 2008). Targeting a protein which is specifically associated with TNBC progression provides a basis for stratified medicine by identifying cohorts of patients that will respond positively to certain treatment with reduced side-effects. CaMK1D is proposed to be a driver for disease progression in BLBC (Bergamaschi et al., 2008), thus it is a relevant therapeutic target that can be implicated in a target based drug discovery programme. However, an *in vitro* system needs to be generated to test the specificity, effectiveness and potency of the inhibitor in cell-based assays in order to plan for future clinical trials of CaMK1D inhibitors.

5.1 Evaluation of the generated cell-based model system

The physiological level of CaMK1D protein expression in breast cancer subtypes has not been studied in detail, thus a model system consisting of cell lines with three varying CaMK1D expression levels were generated: 1) one with CaMK1D levels knocked down using shRNA, 2) one transfected with empty vector for basal levels of CaMK1D expression in that particular cell line, and 3) one overexpressing CaMK1D to study the significantly increased effect of CaMK1D. This was successfully borne out with lentiviral transfections of two BLBC cell lines of interest, i.e. HCC70 and MDA-MB-231 cells. The current method of generation of these model systems introduces clonal variations in the cells due to the random insertion of the plasmid. Transfected

cells were collectively pooled and used for all the experiments conducted, thus the results are not based on single clones. This is advantageous as it represents a heterogeneous population of cells, which could reflect tumour heterogeneity. The slight discrepancies in 2D cellular morphology could be the result of this clonal heterogeneity and the variation in cell cycle status at the time they were photographed. To avoid this, cells should be subjected to serum starvation overnight, inducing cell cycle arrest (Mengfei et al., 2012). This synchronizes the cell cycle status of the cells, allowing the analysis of the consensus morphology. Nonetheless, CaMK1D overexpressing cells predominantly grew in tight cohesive colonies with cells growing layers upon each other whereas CaMK1D knockdown resulted in the formation of a monolayer with flattered cells. This dominant phenotype suggests that CaMK1D expression alters cellular morphology and was the initial indicator that both cell lines of interest were successfully transfected, as was then confirmed by western blot analysis. The shRNAs chosen had effectively downregulated CaMK1D expression in the MDA-MB-231 cells whilst the HA-tagged CaMK1D resulted in an approximately 19-fold increase in CaMK1D expression.

High-grade and poorly-differentiated tumours reportedly have numerous mutations; this greater genomic instability allows for sub-populations of tumour clones to develop drug resistance (Shaw and Johnson, 2012). This can be the result of the target mutation within the patient or resistant-cancer stem cells within the tumour (Hoelder et al., 2012), as demonstrated with the anaplastic lymphoma kinase inhibitor, Crizotinib (Sasaki et al., 2011). In this case, the issue was tackled by discovering a coexisting therapeutic target and thus, the optimal form of therapy was to administer two inhibitors simultaneously. This exemplifies the importance of varying drug administration along the course of the treatment to counter the emergence of drug resistance.

Once another disease driver is identified in such TNBCs, this approach can be adaptable using this type of model system; panels of stably transformed lines can be engineered to express varying levels of another protein. This model system also addresses the issue of off-targets of kinase inhibitors, which tend to be only partially selective. In the case of CaMK1D inhibitors, tests in cells overexpressing only CaMK1D should reflect the primary inhibitory activity against CaMK1D unless the cells also inadvertently overexpress off-targets such as the other CaMK1 isoforms.

These model systems were generated with breast cancer lines harbouring several deregulated proteins, thus, this variation hinders the ability to study the direct effects of CaMK1D. The HCC70 cell line has been associated with increased cell cycle and cell division components (Lehmann et al., 2011). PTEN is a well-known tumour suppressor that regulates the Akt/PKB signalling pathway required for cell survival; aberrant PTEN expression prevents cell cycle arrest and evasion of apoptosis. TP53 codes for another tumour suppressor, the p53 protein, which is also involved in cell cycle regulation. Since these mutations also act as drivers for constitutive cell proliferation, the intrinsic effect of CaMK1D and CaMK1D-specific inhibitors could be masked by the aberrant signalling from other pathways, which may vary between cell lines. The success of Glivec in cells expressing mutant Abl kinase was largely due to the modulation of the oncogenic target kinase by a singly mutant pathway. Thus, it is insufficient to study inhibitor models based solely on tumorigenic cell lines. A cell-based model system from an inherently non-tumorigenic immortalised cell line, for example, MCF-10A, should be also tested. This cell line share features of these BLBCs such as being an adherent mammary epithelial cell line. Optimisation of the small molecule CaMK1D inhibitors could be carried out initially in

transfected MCF-10A cell lines, and the analysis could then be compared to the TNBC model systems generated here. Not only can these model systems provide a platform to these the biological effects of CaMK1D *in vitro*, a series of molecular biomarkers could be delineated. This has a translational aspect as well since these biomarkers could aid patient stratification.

5.2 Identification of potential biomarkers

To provide useful molecular readout of the inhibitor's efficacy, biomarkers that report on the cellular activity of the target need to be validated. These would often be the downstream substrates of the target, however, the exact signalling pathway(s) of CaMK1D remain unclear. Nonetheless, BLBCs have demonstrated mutations in numerous proteins related to the Ras-Raf-MEK-ERK pathway, such as KRAS, BRAF and EGFR（Cancer Genome Atlas Network, 2012). The B-Raf protein is a Ser/Thr kinase, which regulates several cellular processes such as cell division and differentiation. The KRAS protein is a GTPase and functions as an oncogene by propagating signals from proteins like c-Raf. As a result of Ras mutation, an increase in ERK1/2 activity is often observed in BLBCs (Giltnane and Balko, 2014). Thus, some of these members could serve as potential biomarkers. Western blot analysis of EGFR demonstrate a 2-fold increase in total EGFR levels upon CaMK1D knockdown and overexpression. However, these bands appear to be 'fuzzy' or diffused bands suggesting that glycosylation has occurred. It is possible that the protein displays enhanced glycosylation with CaMK1D overexpression, whereas there is an increase in the EGFR protein levels upon CaMK1D knockdown, or vice versa. A well-established method of detecting glycoproteins is to use glycan-binding lectins conjugated to fluorophores (Cummings and Etzler, 2009) that can then be quantified for analysis. This

technique can delineate the differences between protein expression and glycosylation in the bands. However, due to the mesenchymal nature of MDA-MB-231 cells, it has been demonstrated that its EMT nature is the result of hepatocyte growth factor/scatter factor (HGF/SF) and not due to EGF (Trusolino et al., 2000). Even though HGF/SF indirectly activates the Ras-Raf-MEK-ERK pathway, the effects on the c-MET receptor instead of EGFR signalling should be considered.

It has also been reported that CaMK1 mediates the activation of ERK upon the calcium-dependent depolarization of neuroblastoma NG108 cells (Schmitt et al., 2004), suggesting that CaMK1D overexpression would lead to an increase in ERK activity. Although the phosphorylated forms of ERK1/2 were not analysed, protein expression of ERK1/2 observed in our MDA-MB-231 model system suggested a possible contradiction. The western blot analysis of MEK1/2 and ERK1/2 protein expression demonstrated an inverse correlation with CaMK1D expression, suggesting the presence of a possible compensatory mechanism. This could occur at the transcriptional level, where CaMK1D affects the transcriptional machinery involved in expressing MEK1/2 and ERK1/2. Alternatively, at the proteomic level, CaMK1D could trigger the degradation of these proteins via the ubiquitin-proteasome degradation machinery. It has been observed in A431 human epidermoid carcinoma cells that ERK1/2 ubiquitination and subsequent degradation is modulated by MEKK1 upon sorbitol induction (Lu et al., 2002). Similarly, the glycosylation status of EGFR in the MDA-MD-231 model system could target this degradation pathway. CaMK1D overexpression also led to a decrease in c-Raf and p-38 MAPK whereas no significant change was observed at basal and knockdown levels. This suggests that there could be a potential threshold of CaMK1D that is tolerated by the cells before its expression results in a

decrease of these selected MAPK proteins by a similar mechanism to the reduction of the MEK1/2 and ERK1/2 protein expression. Nonetheless, MDA-MB-231 cells are associated with BRAF, CDKN2A, KRAS, NF2, TP53 and PDGFRA mutations (Lehmann et al., 2011). Thus, a conclusive schematic or mechanism of action of the CaMK1D and Ras-MEK pathway cannot be derived by characterising CaMK1D in the background of these mutations. Members of the MAPK/ERK pathway may not serve as useful specific biomarkers because they are often implicated in TNBCs, however, targets of these pathway could be studied to delineate the CaMK1D signalling pathway.

Bergamaschi and colleagues suggested that overexpression of CaMK1D in MCF-10A cells led to increased vimentin levels and increased cell migration, hence, proposed that CaMK1D is involved in EMT. However, they had performed these cell-based assays with a single clone of CaMK1D overexpressing cells. In contrast, our studies revealed no significant changes in vimentin and E-cadherin expression, which was expected due to the inherent mesenchymal nature of MDA-MB-231 cells. Bergamaschi and colleagues also proposed CREB to be a downstream substrate of CaMK1D. Not only has immunoprecipitation analysis demonstrated that CaMK1D phosphorylates CREB *in vitro*, KCl depolarization in CaMK1D overexpressing cells induces an increase in CREB activity (Sakagami et al., 2005). This contradicts our western blot data from which we propose that CaMK1D knockdown and overexpression result in a decrease of phosphorylated CREB. This could be the result of three mechanisms of action. 1) CREB is suggested to be dephosphorylated by PTEN, a phosphatase, which is known to be implicated in MDA-MB-231. CaMK1D knockdown could result in lower levels of phosphorylated PTEN, thereby increasing its activity (Ross and Gericke, 2009). The PTEN enzyme can then

dephosphorylate CREB. 2) Calpain is a calcium-dependent cysteine protease known to be expressed in abundance in MDA-MB-231 (Hu et al., 2010). CaMK1V is thought to be a downstream effector of calpain. Cellular depolarization and calcium-dependent decrease of CaMK1V activity resulted in a 10-fold decrease in phosphorylated CREB (Hu et al., 2010). Thus, CaMK1D overexpression could affect the activity of calpain, causing a decrease in CREB phosphorylation. 3) Phosphorylation of Ser133 on CREB results in CREB activation, which is proposed to be mediated by CaMKII, CaMKIV (Sun et al., 1994) and more recently, CaMK1D (Bergamaschi et al., 2008). Earlier studies of CREB activation demonstrated that CaMKII-mediated phosphorylation of Ser142 on CREB inhibits CREB activation. Thus, Ser142 serves as a negative regulatory site (Sun et al., 1994). Similarly to the ability of CaMKII to phosphorylate both sites, Ser133 and Ser142, CaMK1D could be speculated to phosphorylate Ser142. The antibody used in our analysis was specific for phospho-Ser133 on CREB, thus this theory could be tested using antibodies targeting phosphorylated forms of Ser142.

It has recently been discovered that the scaffolding protein, syntenin-1, correlates to poor patient outcome in TNBC (Yang et al., 2013). Since syntenin has Ser residues that could potentially be directly phosphorylated by the kinase activity of CaMK1D, it was studied by western blot analysis. CaMK1D expression levels correlated inversely with the protein expression levels of syntenin-1 and phosphorylated Ser and Tyr residues on syntenin-1. Since CaMK1D cannot phosphorylate Tyr residues, this mechanism of action is proposed to be indirect, i.e. CaMK1D may interact with another protein that leads to phosphorylation of syntenin-1. Nonetheless, syntenin-1 could be a potential biomarker and should to be analysed across other model systems, for example, HCC70, to identify cell-line specific effects.

To identify substrates phosphorylated on Ser/Thr residues that could correlate with CaMK1D expression, we analysed the levels phosphorylated Ser and Thr residues across the MDA-MB-231 panel of transformed cell lines. Two phosphorylated Ser bands displayed an increase with CaMK1D knockdown and a decrease with CaMK1D overexpression. One band was observed between 37 and 50kDa, which could correspond to phosphorylated Ser 217/221/298 on MEK1/2 since total protein levels of MEK1/2 followed similar distribution. The other phosphor-Ser band was observed below 37kDa, which could correspond to syntenin-1 as observed from our phosphor-Ser specific syntenin-1 antibody. Since these antibodies were not protein-specific, this is an insensitive method of detecting phosphorylated proteins. Each band could represent more than one protein with potential Ser/Thr sites. These bands should be analysed by mass spectrometry to identify the protein(s).

The most well-established substrate of CaMK1D is CDK9. CaMK1D depletion and inhibition of other members of the CaMK cascade have been demonstrated to downregulated the phosphorlyation of the CDK9 T loop (Ramakrishnan and Rice, 2012). Commercially available antibodies suggest that phosphorylation of Thr29 or Thr186 only CDK9 would result in band at approxiamtely 42kDa. Since our western blot analysis of phosphorylated Thr resulted in a band just below 37 kDa, it is unlikely that our non-specific Thr antibodies detected the phosphorylated forms of CDK9. To study this, phospho-CDK9 specific antibodies should be tested. However, phospho-Ser bands were observed between 37 and 50 kDa and there are several other established phosphorylation sites on CDK9, such as Ser175 (Mbonye and Karn, 2014). This residue is an indirect downstream target of the Src pathway via PKC phosphorylation (Joseloff et al., 2002). Thus, another avenue to explore for potential biomarkers is members of the Src pathway.

A conclusive biological mechanism of action of CaMK1D cannot yet be derived from these analyses because the generation of these whole cell lysates and western blot analysis were only performed once. This process needs to be conducted at least two more times before conclusions can be convincingly established. Additionally, total protein levels are not reflective of the phosphorylated states of these proteins and subsequently, the proteins' activity. It would also be appropriate to understand the wider number of pathways which are targeted by these inhibitors of CaMK1D. Western blot analysis of, for example, the members of the Akt/PKB and the apoptotic pathway, after cells have been subjected to the inhibitors should be performed. This would provide a more detailed understanding of overall cellular mechanism of action of the inhibitors.

5.3 Inhibitor testing in cell-based assays

In vitro screening studies of have identified kinase inhibitors with nanomolar affinities for the CaMK family of kinases (Remsing et al., 2009; Anastassiadis et al., 2011; Davis et al., 2011). Fragments of these compounds that retain efficient high affinity for CaMK1D can in principle be combined and merged to generate novel CaMK1D-specific inhibitors. One such compound, GSK-3 XIII, has been studied by Stefan Knapp's and Michael Overduin's labs using X-ray crystallography and NMR spectroscopic methods, showing an affinity of K_D of approximately 1µM for the ATP binding region, thus locking CaMK1D in an autoinhibitory state. Although GSK-3 XIII was originally synthesized to target glycogen synthase, structural understanding of the backbone of this inhibitor and *in vitro* analysis of the compound in these cell based systems provides a foundation for the design of a novel cell-permeable CaMK1D-specific inhibitor.

The initial GSK-3 XIII inhibitor dose effect was tested on the HCC70 panel of transformed cell lines. An approximate 2-fold increase in IC_{50} value was observed with CaMK1D overexpression (IC_{50} value = 11.232 µM) in HCC70 compared to the knockdown cells (IC_{50} value = 4.035µM). This was expected with a CaMK1D-specific inhibitor as an increased inhibitor concentration would be required to target a higher level of target expression. However, the experiment was only carried out once because HCC70 cells were technically hard to maintain due to their limited growth. Nonetheless, it was elucidated from this assay that 10µM of inhibitor would be suffice to perform cytotoxicity assays. An overall decrease in cell proliferation was observed in the MDA-MB-231 model system upon exposure to 10µM of GSK-3 XIII under optimal and sub-optimal serum conditions. It is unclear if the effect was due to cell death or cytostasis. However, the difference between the three stably transfected cell lines was not significant. This suggests that GSK-3 XIII targeted a protein involved in cell proliferation, which was not CaMK1D and growth factors present in the serum did not contribute to proliferative ability of the cells. Furthermore, no significant difference was observed in migration upon the exposure of the MDA-MB-231 model system to GSK-3 XIII. Altogether, this preliminary data suggests that GSK-3 XIII is not a CaMK1D-specific inhibitor in this cell type.

5.4 Evaluation of the cell-based assays established to assess CaMK1D function *in vitro*

Studies have shown that CaMK1D can be activated with Ca^{2+} and CaM binding yet without the Thr phosphorylation by CaMKK. Although CaMK1D is capable of sustaining a partially active state at steady-state conditions, a 1.5-fold increase in CaMK1D activity has been demonstrated with ionomycin stimulation (Ishikawa et al., 2003). The experiments conducted here were performed under steady state conditions, thus, it is possible that there were insufficient calcium

stores to activate the high non-physiological CaMK1D levels in the CaMK1D overexpression transformed line. Although western blot analysis confirm the protein expression of CaMK1D, the experiments conducted so far may not reflect the CaMK1D activity. Comparison with a cell line transfected with a CaMK1D kinase dead mutant might provide insights to the cellular CaMK1D activity, however the mutant itself may alter several unknown signalling pathways. To tackle this issue, the cell-based assays could be carried out simultaneously with and without calcium stimulation, which can be achieved with ionomycin treatment.

Our western blot analysis has suggested that the CaMK1D overexpression is significantly above the physiological levels. Yet, this exceedingly high CaMK1D overexpression did not exhibit responses reflective of inhibition upon the exposure to the GSK-3 XIII inhibitor. One possibility is that the effect of CaMK1D in 2D cell-based assays could be subtle. Differences in cellular morphology of the MDA-MB-231 model system in our 3D culture suggest that CaMK1D can be studied in a more physiological environment. Culturing cells in 3D matrigel does not completely recapitulate the intricacies of a tumour microenvironment, for example, the angiogenic network or the evasion of the immune system, yet it captures the nutritional and gaseous gradient of a physiological tumour niche - the substrate, oxygen, carbon dioxide and waste availability (Fischbach et al., 2007). It also reflects the tumour heterogeneity in terms of gene expression patterns as epigenetic changes could also be result of selection pressure present in physiological environments. This is absent in a 2D plastic cell culture, which develops in a highly uniform environment. The apical-basal polarity of proteins modifies not only the morphology of cells but also the cellular function (Fischbach et al., 2007). Thus, responses to drugs in 2D culture do not necessarily reflect a physiological response. Whereas 2D cultures permit the complete

penetration of drug to cells, under physiological conditions, tumorigenic cells can form in a spheroid mass, in which cells on the outer surface are subjected to the inhibitors whilst those within the spheroid are chemoprotected by those cells. Studies have shown that 3D cultures are more likely to upregulate genes associated with "stemness", hence are likely to reflect the inhibitors' efficacy with cancer stem cells present (Fischbach et al., 2007). Thus, cell-based assays used to analyse the effects of GSK-3 XIII should be performed on 3D cultures of the model system.

5.5 Extended application of CaMK1D-specific inhibitors

According to Waddington's theory of genetic canalization, tumours without any common mutations could affect the same network (Hofree et al., 2013). Not all BLBCs are TNBCs, and vice versa (Cancer Genome Atlas Network, 2012). Thus, these model systems can be generated with other appropriate cell lines. Recently, another breast cancer subtype has emerged, which is known as claudin-low. This name is due to the decreased expression of claudins, which modulate the tight-tight junctions in epithelial cells. These TNBCs exhibit EMT features with increased immune-infiltrate and display enhanced processes associated with "stemness" (Prat et al., 2010). Claudin-low and BLBC are proposed to be more similar regarding their gene expression compared to their counterparts. In fact, MDA-MB-231, has been demonstrated to exhibit a gene expression pattern reflective of the claudin-low breast cancer subtype (Prat et al., 2010). Additionally, both of these TNBCs, claudin-low and BLBC, demonstrate similar patient prognosis (Perou, 2010). Thus, targeting CaMK1D could be extended to patients with claudin-low breast cancer. CaMK1D has also been associated with type-II diabetes, where RNAi studies have suggested that CaMK1D regulates gluconeogenesis and glycolysis regulation in a primary

human hepatocyte model (Haney et al., 2013). Previous cDNA microarray studies have reported CaMK1D downregulation in retinoblastoma tissues (Chakraborty et al., 2007). Another study have reported that deletion of the 10p13 chromosomal region was commonly observed in childhood neuroblastoma (Altura et al., 1997). The understanding of CaMK1D biological significance and the generation of a CaMK1D-specific drug would not only benefit breast cancer patients, it could be applicable to other health conditions.

6. Conclusion

In conclusion, the CaMK1D-specific model system established here using mammary tumorigenic cell lines is an appropriate preliminary system for the evaluation of potential CaMK1D-specific inhibitors using cell-based assays, which include western blot analysis of signalling biomarkers, cytotoxicity analysis and wound healing experiments. Potential novel CaMK1D biomarkers, such syntenin-1, have been identified in the preliminary analyses of the MDA-MB-231 model system. Nonetheless, phosphorylated forms of other potential biomarkers need to be analysed to determine cellular protein activity. Cytotoxicity and migration assay of the MDA-MB-231 model system exposed to the primary inhibitor of interest, GSK-3 XIII, demonstrated that its toxicity was not CaMK1D-specific although the numerous tumorigenic mutations inherent in MDA-MB-231 cells could mask this potential CaMK1D-specific inhibitory effect. Thus, this type of model system should also be generated with a non-tumorigenic immortalised cell line, for example, MCF-10A, to validate this theory. Further modifications to this model system are required prior to high throughput testing of the *in vitro* inhibitory effects of small molecule compounds, but the system is now appropriate for analysis of the cellular activities and signalling effects of pilot sets of CaMK1D inhibitors.

7. References

Altura, R.A., Maris, J.M. and Li, H. et al. (1997) Novel regions of chromosomal loss in familial neuroblastoma by comparative genomic hybridization. **Genes Chromosomes Cancer,** 19(3):176-184

Anastassiadis, T., Deacon, S.W. and Devarajan, K. et al. (2011) Comprehensive assay of kinase catalytic activity reveals features of kinase inhibitor selectivity. **Nat Biotechnolo,** 29(11):1039-1045

Badve, S., Dabbs, D.J. and Schnitt, S.J. et al. (2011) Basal-like and triple-negative breast cancers: a critical review with an emphasis on the implications for pathologists and oncologists. **Mod Pathol,** 24 (2): 157-167

Bergamaschi, A., Kim, Y.H. and Kwei, K.A. et al. (2008) CAMK1D amplification implicated in epithelial-mesenchymal transition in basal-like breast cancer. **Mol Oncol,** 2(4):327-339

Berridge, M. J., Bootman M. D. and Lipp, P. (1998) Calcium--a life and death signal. **Nature**, 395(6703): 645-648

Blows, F.M., Driver, K.E. and Schmidt, M.K. et al. (2010) Subtyping of Breast Cancer by Immunohistochemistry to Investigate a Relationship between Subtype and Short and Long Term Survival: A collaborative analysis of data for 10,159 cases from 12 studies. **PLoS Med,** 7(5): e1000279

Cancer Research UK. (2014) **Breast cancer incidence statistics** [online]. Available from: http://www.cancerresearchuk.org/cancer-info/cancerstats/types/breast/incidence/uk-breast-cancer-incidence-statistics#source1. [Accessed 5 August 2014]

Cancer Genome Atlas Network. (2012) Comphrensive molecular portraits of human breast tumours. **Nature**, 490(7418):61-70

Capdeville, R., Buchdunger, E. and Zimmermann, J. et al. (2002) Glivec (STI571, imatinib), a rationally developed, targeted anticancer drug. **Nat Rev Drug Discov,** 1(7):493-502

Chakraborty, S., Khare, S. and Dorairaj, S.K. et al. (2007) Identification of genes associated with tumorigenesis of retinoblastoma by microarray analysis. **Genomics**, 90(3):344-353

Cummings R. D. and Etzler M. E. (2009) **Antibodies and lectins in glycan analysis. Essentials of Glycobiology,** 2nd edition. Cold Spring Harbor (NY): Cold Spring Harbor Laboratory Press.

Curtis, C., Shah, S.P. and Chin, S.F. et al. (2012) The genomic and transcriptomic architecture of 2,000 breast tumours reveals novel subgroups. **Nature,** 486(7403):346-352

Dancey, J. and Sausville, E.A. (2003) Issues and progress with protein kinase inhibitors for cancer treatment. **Nat Rev Drug Discov,** 2(4):296-313

Davis, M.I., Hunt, J.P. and Herrgard, S. et al. (2011) Comprehensive analysis of kinase inhibitor selectivity. **Nat Biotechnolo**, 29(11):1046-1051

Fan, C., Oh, D.S. and Wessels, L. et al. (2006) Concordance among gene-expression-based predictors breast cancer. **N Engl J Med,** 355(6):560-569

Fischbach, C., Chen, R. and Matsumoto, T. et al. (2007) Engineering tumors with 3D scaffolds. **Nat Methods,** 4(10):855-860

Gamboa-Meléndez, M.A., Huerta-Chagoya, A. and Moreno-Macías, H. et al. (2012) Contribution of common genetic variation to the risk of type 2 diabetes in the Mexican Mestizo population. **Diabetes**, 61(12):3314-3321

Giltnane, J.M. and Balko, J.M. (2014) Rationale for targeting the Ras/MAPK pathway in triple-negative breast cancer. **Discov Med,** 17(95):275-283

Hanahan, D. and Weinberg, RA. (2011) Hallmarks of Cancer: The Next Generation. **Cell**, 144 (5):646-74

Haney, S., Zhao, J. and Tiwari, S. et al. (2013) RNAi screening in primary human hepatocytes of genes implicated in genome-wide association studies for roles in type 2 diabetes identifies roles for CAMK1D and CDKAL1, among others, in hepatic glucose regulation. **PLoS One**, 8(6):e64946

Hoeflich, K. P., O'Brien, C. and Boyd, Z. et al. (2009) In vivo antitumor activity of MEK and phosphatidylinositol 3-kinase inhibitors in basal-like breast cancer models. **Clin Cancer Res,** 15(14): 4649-4664

Hoelder, S., Clarke, P.A. and Workman, P. (2012) Discovery of small molecule cancer drugs: Successes, challenges and opportunities. **Mol Oncol**, 6(2):155-176

Hofree, M., Shen, J. and Carter, H., et al. (2013) Network-based stratification of tumor mutations. **Nat Methods**, 10 (11): 1108-1115.

Hook, S. S. and Means, A. R. (2001) Ca(2+)/CaM-dependent kinases: from activation to function. **Annu Rev Pharmacol Toxicol,** 41: 471-505

Hopkins, A.L. and Groom, C.R. (2002) The druggable genome. **Nat Rev Drug Discov,** 1(9):727-730

Hu, J.H., Elliott, B. and Greer, P.A. (2010) Abstract 3269: Calpain knockdown in human breast carcinoma cells reduced xenograft tumor growth rates and inhibited in vitro cell migration and proliferation. **Cancer Res**, 70(8 Supplement): 3269

Ishikawa, Y., Tokumitsu, H. and Inuzuka, H. et al. (2003) Identification and characterization of novel components of a Ca2+ /calmodulin-dependent protein kinase cascade in HeLa cells. **FEBS Lett,** 550(1-3):57-63

Joseloff, E., Cataisson, C. and Aamodt, H. et al. (2002) Src family kinases phosphorylate protein kinase C delta on tyrosine residues and modify the neoplastic phenotype of skin keratinocytes. **J Biol Chem,** 277(14):12318-12323

Kao, J., Salari, K. and Bocanegra, M. et al. (2009) Molecular Profiling of Breast Cancer Cell Lines Defines Relevant Tumor Models and Provides a Resource for Cancer Gene Discovery. **PLoS One**. 4(7): e6146

Kenny, P.A., Lee, G.Y. and Myers, C.A. et al. (2007) The morphologies of breast cancer cell lines in three-dimensional assays correlate with their profiles of gene expression. **Mol Oncol,** 1(1): 84-96.

Kimura, Y., Corcoran, E.E. and Eto, K. et al. (2002) A CaMK cascade activates CRE-mediated transcription in neurons of Caenorhabditis elegans. **EMBO Rep,** 3(10):962-966

Lehmann, BD., Bauer, JA. and Chen, X. et al. (2011) Identification of human triple-negative breast cancer subtypes and preclinical models for selection of targeted therapies. **J Clin Invest,** 121(7): 2750-2767.

Lu, Z., Xu, S. and Joazeiro, C. et al. (2002) The PHD Domain of MEKK1 Acts as an E3 Ubiquitin Ligase and Mediates Ubiquitination and Degradation of ERK1/2. **Mol Cell**, 9(5):945-956

Majorano, E., Regan, M.M. and Viale, G. et al. (2010) Prognostic and predictive impact of central necrosis and fibrosis in early breast cancer. Results from two International Breast Cancer Study Group randomized trials of chemoendocrine adjuvant therapy. **Breast Cancer Res Treat,** 121(1):211-218

Manning, G., Whyte, D. B. and Martinez, R. et al. (2002). The protein kinase complement of the human genome. **Science,** 298(5600): 1912-1934

Means, A. R. (2000). Regulatory cascades involving calmodulin-dependent protein kinases. **Mol Endocrinol,** 14(1): 4-13

Mengfei, C., Jingjing, H. and Xuejiao, Y. et al. (2012) Serum Starvation Induced Cell Cycle Synchronization Facilitates Human Somatic Cells Reprogramming. **PLoS One,** 7(4): e28203

Mbonye, U. and Karn, J. (2014) Transcriptional control of HIV latency: Cellular signaling pathways, epigenetics, happenstance and the hope for a cure. **Virology**, 454-455:328-339

Perou, C.M. (2010) Molecular Stratification of Triple-Negative Breast Cancers. **Oncologist**, 15 Suppl 5:39-48

Perou, C.M., Sørlie T. and Eisen M.B. et al. (2000) Molecular portraits of human breast tumours. **Nature**, 406 (6797):747-752

Prat, A., Parker, J.S. and Karginova, O. et al. (2010) Phenotypic and molecular characterization of the claudin-low intrinsic subtype of breast cancer. **Breast Cancer Res,** 12:R68

Rakha, E.A., Reis-Filho, J.S. and Ellis, I. O. (2008) Basal-Like Breast Cancer: A Critical Review. **J Clin Oncol,** 26 (15): 2568-2581

Ramakrishnan, R. and Rice, A.P. (2012) Cdk9 T-loop Phosphorylation Is Regulated by the Calcium Signaling Pathway. **J Cell Physiol,** 227(2):609-617

Remsing, Rix. L.L., Rix, U. and Colinge, J. et al. (2009) Global target profile of the kinase inhibitor bosutinib in primary chronic myeloid leukemia cells. **Leukemia**, 23(3):477-485

Rinnab, L., Schütz, S.V. and Diesch, J. et al (2008) Inhibition of glycogen synthase kinase-3 in androgen responsive prostate cancer cell lines: are GSK inhibitors therapeutically useful?. **Neoplasia**, 10(6):624-34

Rodriguez-Mora, O. G., LaHair, M. M. and McCubrey, J. A. et al. (2005) Calcium/calmodulin-dependent kinase I and calcium/calmodulin-dependent kinase kinase participate in the control of cell cycle progression in MCF-7 human breast cancer cells. **Cancer Res,** 65(12):5408-5416

Ross, A.H. and Gericke, A. (2009) Phosphorylation keeps PTEN phosphatase closed for business. **Proc Natl Acad Sci U S A,** 106(5):1297-1298

Sakagami, H., Kamata, A. and Nishimura, H. et al. (2005) Prominent expression and activity-dependent nuclear translocation of Ca2+/calmodulin-dependent protein kinase Idelta in hippocampal neurons. **Eur J Neuro,** 22(11):2697-2707

Sala-Valdés, M., Gordón-Alonso, M. and Tejera, E. et al. (2012) Association of syntenin-1 with M-RIP polarizes Rac-1 activation during chemotaxis and immune interactions. **J Cell Sci,** 125 (5): 1235-1246

Sasaki, T., Koivunen, J. and Ogino, A. et al. (2011) A novel ALK secondary mutation and EGFR signaling cause resistance to ALK kinase inhibitors. **Cancer Res**, 71(18):6051-6060

Schmitt, J.M., Wayman, G.A. and Nozaki, N. et al. (2004) Calcium Activation of ERK Mediated by Calmodulin Kinase I. **J Biol Chem,** 279(23):24064-24072

Shaywitz, A.J. and Greenberg, M. E. (1999) CREB: a stimulus-induced transcription factor activated by a diverse array of extracellular signals. **Annu. Rev. Biochem**, 68:821–861

Shaw, E. and Johnson, P. (2012) Stratified medicine for cancer therapy. **Drug Discov Today,** 17(5): 261-268

Soderling, T. R. (1999). The Ca-calmodulin-dependent protein kinase cascade. **Trends Biochem Sci,** 24(6): 232-236

Soderling, T. R. and Stull, J. T. (2001) Structure and regulation of calcium/calmodulin-dependent protein kinases. **Chem Rev,** 101(8): 2341-52

Sun, P., Enslen, H. and Myung. P.S. et al. (1994) Differential activation of CREB by Ca2+/calmodulin-dependent protein kinases type II and type IV involves phosphorylation of a site that negatively regulates activity. **Genes Dev,** 8(21):2527-2539

Suzuki, K., Hata, S. and Kawabata, Y. et al. (2004) Structure, Activation, and Biology of Calpain. **Diabetes.** 53(1): 12-18

Swulius, M.T. and Waxham, M.N. (2008) Ca(2+)/Calmodulin-dependent protein kinases. **Cell Mol Life Sci,** 65(17):2637-2657

Takahashi-Yanaga, F. (2013) Activator or inhibitor? GSK-3 as a new drug target. **Biochem Pharmacol,** 86(2):191-199

Toft, DJ. and Cryns, VL. (2011) Minireview: Basal-like breast cancer: from molecular profiles to targeted therapies. **Mol Endocrinol,** 25(2): 199-211

Tong, M. (2011) Evaluation of Protein Kinases for Solution NMR Spectroscopy and the Structural Mechanism of Inhibition and Activation of an Oncogenic Calcium Calmodulin Dependent Protein Kinase. PhD thesis, University of Birmingham

Tremper-Wells, B. and Vallano, M.L. (2005) Nuclear Calpain Regulates Ca^{2+}-dependent Signaling via Proteolysis of Nuclear Ca^{2+}/Calmodulin-dependent Protein Kinase Type IV in Cultured Neurons. **J Biol Chem,** 280: 2165-2175

Trusolino, L., Cavassa, S. and Angelini, P. et al. (2000) HGF/scatter factor selectively promotes cell invasion by increasing integrin avidity. **FASEB J,** 14(11):1629-1640

Verploegen, S., Lammers, J. W. and Koenderman, L. et al. (2000) Identification and characterization of CKLiK, a novel granulocyte Ca(++)/calmodulin-dependent kinase. Blood, 96(9): 3215-3223

Verploegen, S., Ulfman, L. and van Deutekom, H. W. et al. (2005). Characterization of the role of CaMKI-like kinase (CKLiK) in human granulocyte function. **Blood**, 106(3): 1076-83

Wang, X., Pankratz, V.S. and Fredericksen, Z. et al. (2010) Common variants associated with breast cancer in genome-wide association studies are modifiers of breast cancer risk in BRCA1 and BRCA2 mutation carriers. **Hum Mol Genet,** 19 (14): 2886-2897

Yang, Y., Hong, Q. and Shi, P. et al. (2013) Elevated expression of syntenin in breast cancer is correlated with lymph node metastasis and poor patient survival. **Breast Cancer Res,**15(3):R50